

Story of our Universe

Bijay Kumar Sharma*

B.TECH, MS (Stanford), PhD (Univ.of Maryland), Retired Professor, National Institute of Technology, India

*Corresponding Author

Bijay Kumar Sharma, MS(Stanford), PhD (Univ.of Maryland), Retired Professor, National Institute of Technology, India.

Submitted: 2023, Dec 01; Accepted: 2024, Jan 23; Published: 2024, Jan 31

Citation: Sharma, B. K. (2024). Story of our Universe. *J Math Techniques Comput Math*, 3(1), 01-44.

Abstract

Story of our Universe is divided into four major chapters: Before the Big-Bang, at the Big-Bang followed by Inflationary Phase, end of inflationary phase followed by decelerating expansionary phase, point of inflexion, start of accelerating expansionary phase followed by cold death/bouncing Universe/big crunch.

Milestones of Modern Astronomy

Year	Milestone Event
1054CE	Crab Supernova
1609CE	Galileo builds first telescope
1655CE	Newton describes Gravity
1905CE	Einstein Publishes his landmark paper on Relativistic Gravity
1929CE	Hubble Law Propounded
1950CE	QUASER discovered
1964CE	CMBR discovered by Wilson and Panzias
1957CE	Pulsar Star discovered and S.Chandrshekher and his theory on Neutron Star vindicated
1987CE	SN1987A detected by Ian Shelton.This event had occurred 170,000years ago
1990CE	Hubble telescope was launched and a new era began in Observational Astronomy
1990CE	COBE confirms the anisotropy in CMBR thereby vindicating Big Bang Theory propounded by George Gamow.
1993CE	Hubble Space Telescope repaired

Before going to our main discourse I will briefly dwell on the achievement of S. Chandrshekher who wrote his master piece for his doctoral thesis in 1929 and was awarded a Nobel Prize for the same in 1987.

In 1926, Pauli Exclusion Principle and Fermi-Dirac Statistics were proposed. Both these principles were applied by R.

H. Fowler (1926) to the dead star left over from the Novae Explosion of a Red Giant. He proposed the concept of White Dwarf (WD) which has unusually high matter density as is evident from Table 1. He correctly pointed out that at the high matter density observed in WD, electron degenerate pressure will stop the further gravitational collapse. He considered electrons to be Fermi-gas but non-relativistic.

Material	$\rho(\text{kg/m}^3)$	Note	Reference
Water(fresh)	1000	STP	
Osmium	22,610	300K	
WD	10^9		Johnson(2007)
Atomic Nucleus	2.3×10^{17}	Not a strong function of the size	Nave(2009)
Neutron Star	8.4×10^{16} to 1×10^{18}		
Black Hole	2×10^{30}	Critical density of Earth mass BH	Adams(1997)

Table 1. Comparative study of the matter density (ρ) of different celestial objects

Subsequently Chandrashekher (1930) [Srinivas (1997)] applied special theory of relativity to the Fermi Gas of Electrons in White Dwarf. As seen in Figure 1, if the Fermi Electron Gas is treated as relativistic gas then addition of mass leads to a mass limit of $1.44M_{\odot}$ where White Dwarf has a equivalent radius of Zero. This means the collapse becomes a free fall. This means WD cannot exist at $1.44M_{\odot}$. Chandrashekher concluded that at this mass limit WD will exist as Neutron Star(NS) where neutron degenerate pressure will stop the gravitational collapse. Thus the hypothesis of the existence of NS was put forward.

This was finally vindicated when the British astronomer Jocelyn Bell Burnell discovered pulsars while completing her PhD at Cambridge University in 1967. Using a radio telescope designed by her advisor Anthony Hewish and Martin Ryle (both men later shared a Nobel prize for their work), Bell Burnell found strange radio pulses coming from a single point in the sky. After a period of confusion about what was causing the pulses, Bell Burnell and her colleagues confirmed that pulses are emitted by rapidly spinning neutron stars called Pulsars as the sources of pulses came to be known.

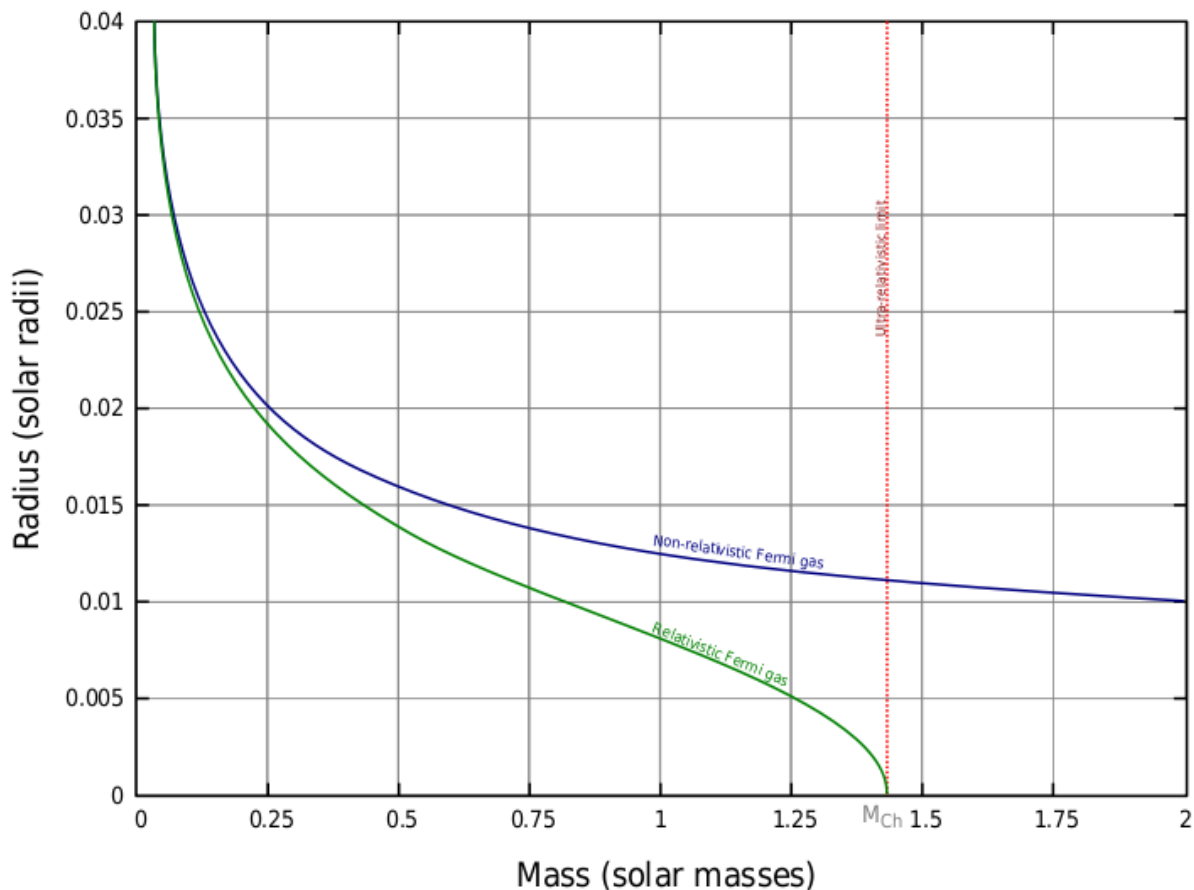


Figure 3. Radius–mass relations for a model white dwarf. M_{limit} is denoted as M_{Ch}

[It shows how radius varies with mass for non-relativistic (blue curve) and relativistic (green curve) models of a white dwarf. Both models treat the white dwarf as a cold Fermi gas in hydrostatic equilibrium. The average molecular weight per electron, μ_e , has been set equal to 2. Radius is measured in

standard solar radii and mass in standard solar masses. Adapted from Chandrashekher,S.; “The Highly Collapsed Configuration of Stellar Mass”, Monthly Notices of Royal Astronomical Society of London, 95, (1935),pp.207-225]

1. Chapter 1- Before the Big-Bang

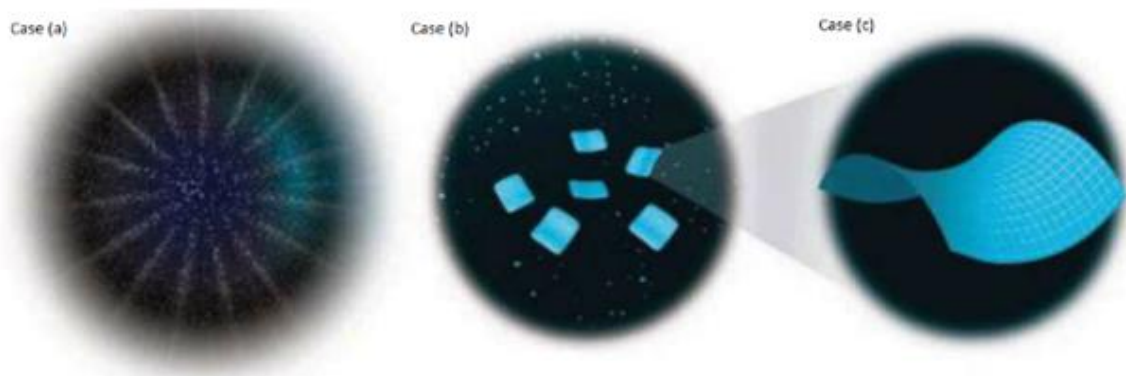


Figure 3. Case (a) “The Big-Bang was sparked when quantum fluctuation in the Metaverse caused a New Universe to pop-up into being like an air-bubble in the boiling water”.

Case (b). “Within the Metaverse, other bubble Universes are being born. Each one expands at the speed of light”.

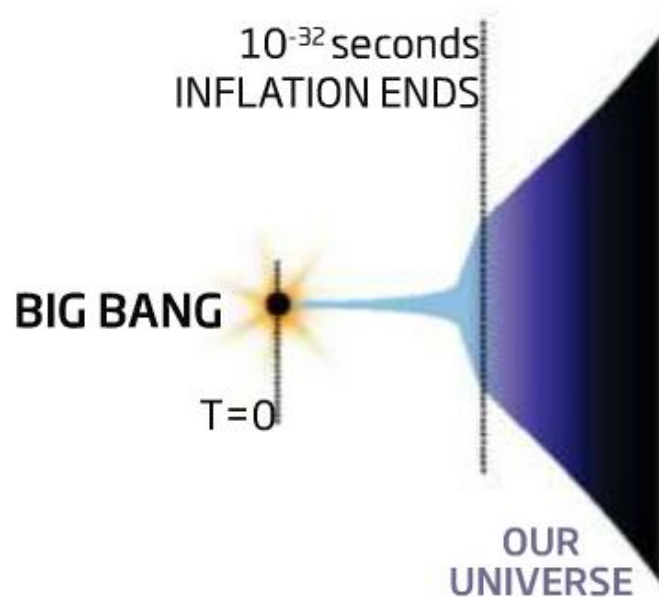
Case (c) “Each Bubble Universe has a lower energy density than the surrounding Metaverse which means Space-Time Fabric takes on a saddle shape”. [Fractal 89.eps]

We live in multi-Universe called Metaverse. Metaverse is populated with large number of universes popping up. Each Universe popping up is like a Big-Bang of the given Universe. Our Universe underwent a similar fate. Our Universe also popped up like a bubble in the boiling water. Our Universe expands initially at a speed greater than light. Gravitational Energy density profile corresponding to our Universe is lower

compared to the surrounding Energy Density profile of the metaverse. Our Universe as a whole is sitting in a Gravitational Potential Energy Valley and in the process acquiring a Saddle shaped curvature (super-curvature) as shown in Figure 3 though in our local Universe WMAP and Planck studies have detected Flat Universe with near-zero curvature. This super-curvature will play a pivotal role in subsequent evolution of our Universe.

STANDARD VIEW

In the big bang model, a single point explodes outwards. The rapid expansion called inflation begins and ends slivers of a second later



Fractal 99.jpg. “Bouncing Baby COSMOS gets a push”, Lisa Grossman,N.S.26th October 2013,pp.10

2. Chapter 2. The Big Bang and the Aftermath

In 1920, our vision of our Universe was confined to the galaxy Milky Way (MW). Edwin Powell Hubble while working on 60 inch telescope on Mount Wilson Observatory, California, USA, discovered that there were many other Galaxies farther beyond Milky Way. The radius of Milky Way, a spiral galaxy, has a radius 50kly= 15.34pc (1parsec or 1pc=3.26ly). By Cepheid Variable stars the distance to the given star or to the given galaxy can be measured. It became the cosmic benchmark for scaling galactic and extra galactic distances. Hubble observed many

small diffuse patches besides the Milky Way. He assumed them to be inside the Milky Way but when he started measuring the distances, he found them much farther than 50kly limits. So he concluded that these patches were independent galaxies lying much beyond MW. He also found that most of the distant stars had their absorption spectrum Red-Shifted which implied that these distant galaxies were receding. He also found that the velocity of recession was directly proportional to the distance d of the galaxy and he put forth the now famous Hubble Law namely:

$$v_{\text{recession}} = d \times H_0 \quad 1$$

where d=distance of the receding object and H_0 =Hubble Constan.

$$d = \frac{c}{H_0} \left[\frac{(z+1)^2 - 1}{(z+1)^2 + 1} \right] \quad 3$$

Velocity of Light in free space = c = 299792458 m/s and Hubble Constant as determined by Planck's probe is $H_0 = 67.164(\text{km/s})/$

Mpc = $2.1764 \times 10^{-18}/\text{sec}$. So the final definitive Age of our Universe:

$$\text{Age of our Universe} = \frac{1}{H_0} = \frac{1}{2.3 \times 10^{-18}} \text{ sec} = 4.59472 \times 10^{17} \text{ sec}$$

We measure Age of Universe in Solar Years and

$$1 \text{ Solar Year} = \frac{365.25 \text{ days (Julian Calender)}}{\text{solar - year}} \times \frac{24 \text{ h}}{\text{d}} \times \frac{3600 \text{ s}}{\text{h}} = 31.5576 \times \frac{10^6 \text{ s}}{\text{y}} \quad 5$$

By combining (4) and (5), Age of our Universe is:

$$\text{Hubble Time} = \text{Age} = 4.59472 \times \frac{10^{17}}{31.5576 \times 10^6} \text{ y} = 14.559 \text{ by} \quad 6$$

Inserting the magnitudes of c and H_0 in (3) we get the answer in meters which is:

$$d = 14.559 \left[\frac{(z+1)^2 - 1}{(z+1)^2 + 1} \right] \text{ bly} \quad 7$$

Seria l	z(red-shift)	d(ly)	Time from BB	comments	Description of our Universe
3K	0	0	13.822by	Our galaxy	
		170,000 ya			Supernova 1987A exploded and first detected by Ian Shelton in 1987.
		600,000 ya			Homosapiens
		65Mya			Dinosaurs become extinct by meteorite strike on Earth
		200Mya			Mammals evolve
		700Mya			Primitive Animals
	0.125	1.66476b ly	12.1648b y		
	0.26	3.16bly	10.6695b y		

		3.8bya			Earliest life form emerged
Accelerated Expansion starts because now DE dominates					
	0.46	4.92693b ly	8.9by	Cosmic Jerk	Decelerated expansion switched to accelerated expansion
		5bly			Birth of our solar system
	1	7.97489b ly	5.85469b y		
		10bly			Birth of milky way-3 rd gen galaxy
	2	10.5541b ly	3.27544b y	Cosmic High Noon	Star Formation Rate is at its peak
	5	12.6529b ly	1.17067b y	Reionization is completed	H & He plasma is very dilute hence Universe remains transparent
	10	13.3577b ly	471.922 My		
	11.35	13.4329b ly	396.654 My	Half-reionization era	
	16	13.5841b ly	245.478 My	First Generation Stars are born-reionization begins-emerges out of dark age	Densest clumps of density perturbations give birth to the first stars.
4000 K Low-est MH D Temp	1090	13.8291b ly	429,141y	Matter decouples and light released. Cosmic haze is lifted, dark age sets in	First Recombination era. Radiation domination ends. Baryonic Matter starts dominating
	3402	13.8295b ly	66,806y	Dark Matter decouples & evolves into Haloes	Builds Cosmic Web scaffolding on which baryon will clump
			10,000y	Radiation era	
289K			20mins	Nucleosynthesis terminates	
Inflationary phase ends and decelerated expansion starts;DM and BM dominate					
745K	400,000,000 to 200,000,000		3mins	Nucleosynthesis begins	H:He stabilize at 75%:25% by mass

			1s to 3 mins	H and He nuclei stabilize	Lepton Epoch
			3 second	Basic elements formed	Leptons dominate: $e + \text{anti}_e(\text{positron}) \rightarrow \text{photon} \rightarrow e + \text{positrons}$
10^{10} K			1sec		Some residual hadron left Neutrinos decouple
10^{13} K			10^{-6} second	Universe shaped. Hadrons	Quarks are confined to hadrons(doublets+triplets) Neutrinos generated
10^{16} K			10^{-12} s	Quark Epoch, the four forces assume the present form.	By Baryogenesis a surplus of quarks are leftover. This will form the Baryonic matter
10^{22} K			10^{-32} second	Inflationary phase ends - 10^{-33} cm sized Universe blows up to 10cm golf ball instantaneously	Energy released is transferred to our Universe making it a fiery ball
10^{32} K		13.82bly	10^{-43} second	Inflationary phase begins	Decay of false vacuum propels our Universe to exponential expansion
			0 second	BB	

Table 1. 'd' vs z

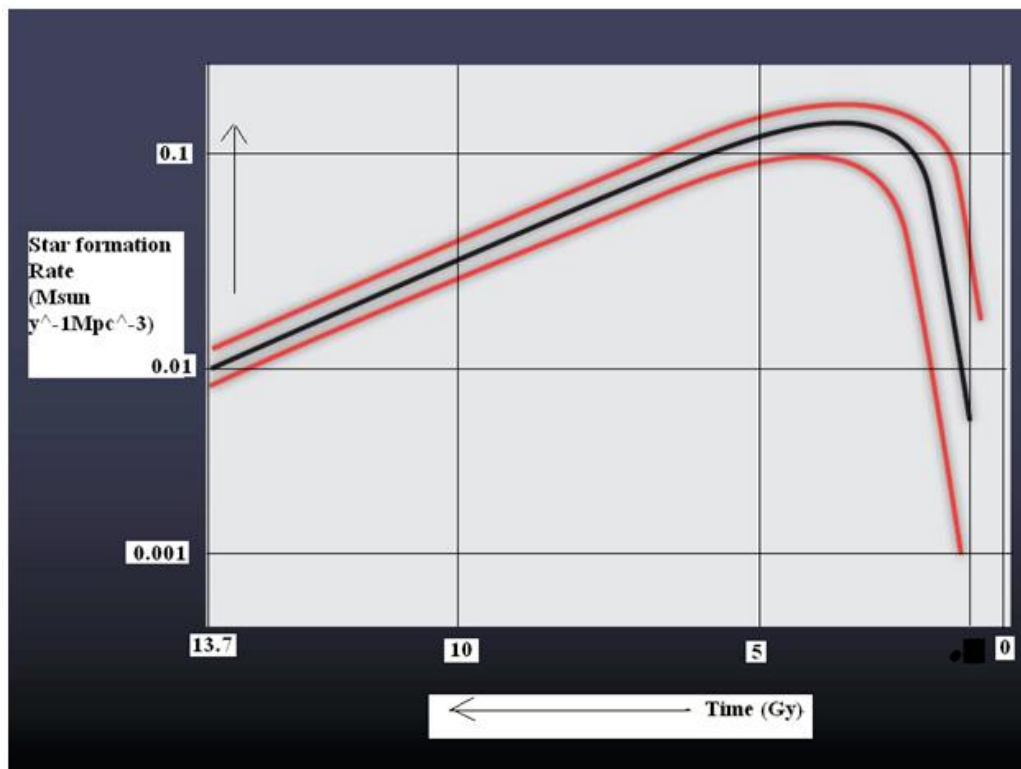


Fig. B.1 A simple representation of our current knowledge of the rise and fall of globally averaged star-formation activity over the 13.7 billion years of cosmic history. The black line indicates our best estimate of how the density of star formation (in solar masses formed per year per unit of co-moving volume) grew rapidly in the first 2 billion years after the Big Bang, stayed roughly constant for a further ~ 2.5 billion years, then has declined almost linearly with time since the universe was ~ 5 billion years old. The red lines indicate the typical current uncertainty in the measurement, which rises to approximately an order of magnitude at the earliest times.

2.1 Big-Bang, Expanding Universe Theory and its Unexplainable Puzzles

From Hubble Law it was concluded that initially when our Universe popped up in Metaverse it must have been squeezed

in an unimaginably hot (10^{32}K) and (10^{94}gm/cc) dense compact object. From this hot and dense fiery ball, our Universe sedately expanded. Infact it was shown that it was a decelerated expansion.

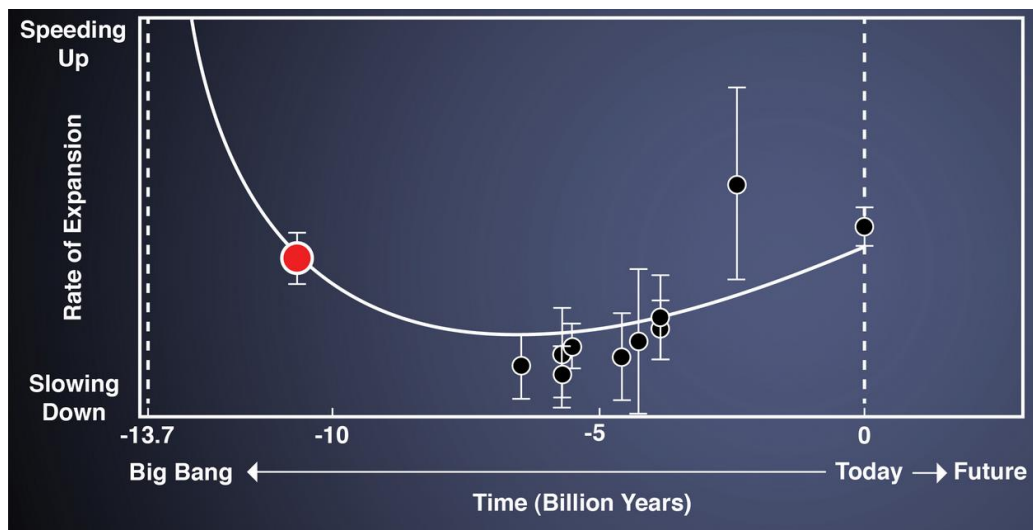


Figure 18. Until recently, three-dimensional maps by BOSS and other surveys were able to measure the regular distribution of galaxies back to an average of only about five and a half billion years ago, a time when the expansion of the universe was already accelerating. BOSS's quasar measurements (red circle, left), by measuring the distribution of intergalactic gas, have now probed the structure of the early universe at a time when expansion was still slowing under the influence of gravity. The quasar data gives new access to the transition from deceleration to acceleration caused by dark energy. (Graph by Zosia Rostomian, Lawrence Berkeley National Laboratory, and Nic Ross, BOSS Lyman-alpha team, Berkeley Lab) [Fractal94].

So BB was not an explosion but the appearance of saddle shaped Space-Time fabric of the observable Universe in a causal patch of much larger unobservable Metaverse. But subsequent experiments and observations showed that “Expanding Universe Model” had three problems. The problems were:

- (1) why photon to baryon ratio $= 10^{10}$ photon per baryon. (See background material- a quick revision of Standard Particle Theory is given).
- (2) why there is no magnetic monopole when GUT phase transition predicts a large abundance of magnetic monopole.
- (3) why Universe appears to be homogeneous and isotropic all over especially from the study of Cosmic Microwave Background Radiation (CMBR) - the origin of CMBR will be given in next section- this is called the horizon problem.
- (4) why our local Universe is remarkably flat because the flatness parameter $\Omega = \text{actual density of (dark matter + baryonic matter + dark energy) / critical density of (dark matter + baryonic matter + dark energy)} = 1$ is highly unstable because of its runaway tendency of ending in a final crunch if $\Omega > 1$ or a final cold death of infinite expansion if $\Omega < 1$.

(5) Origin of density perturbations in CMBR which led to small scale inhomogeneity in form of super-clusters, clusters, galaxies and solar systems and long walls clumping at the nodes and along the filaments of the cosmic web. An illustration of the cosmic web is shown in Figure 4.

(6) Most of all why the popped up hot, dense compact object not collapsed back into oblivion. At the Planck density of 10^{94} gm/cc , popped up Universe should have been entombed in a black hole because Schwarzschild Radius of this compact object is $3.178 \times 10^{-35} \text{ m}$ and is comparable to Planck's length of $1.6 \times 10^{-35} \text{ m}$. There should be a very strong counteracting force which does not only prevent the gravitational collapse but infact kick starts a sedately expanding Universe.

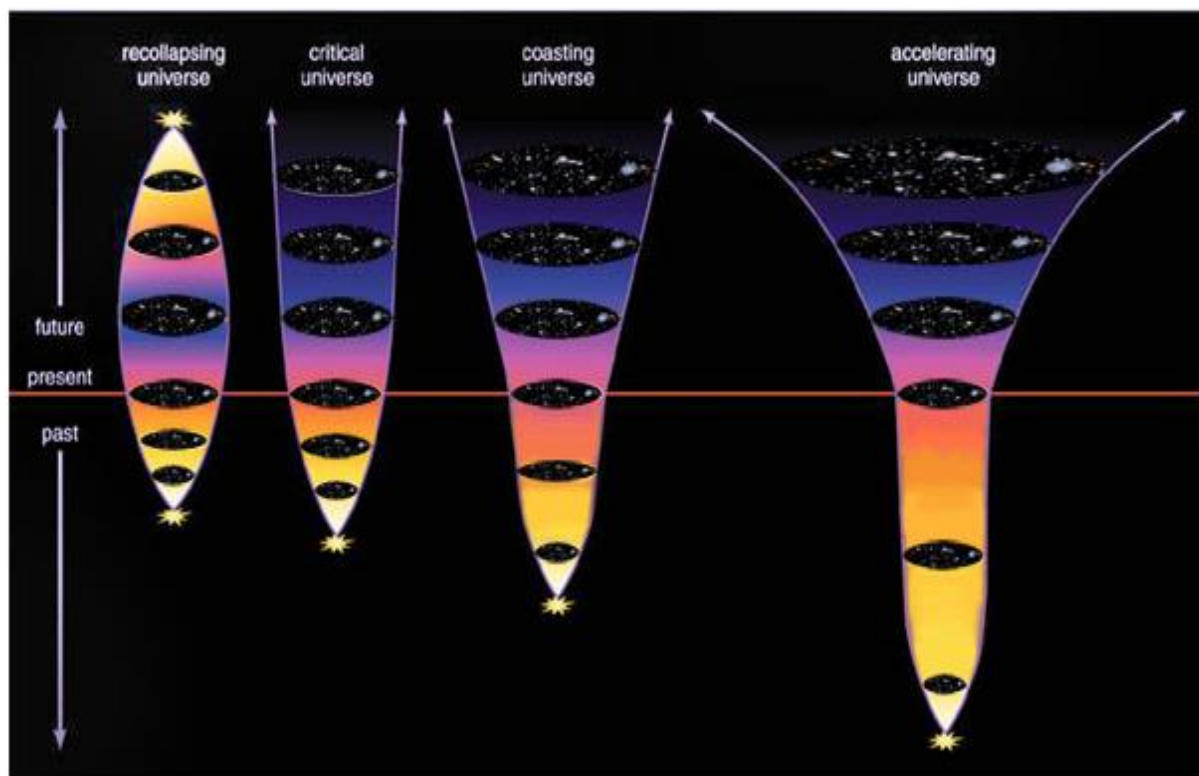


Figure 6. The four scenarios of the possible end of Universe- 1st Scenario $\Omega > 1$ – it is a closed universe and ends in a crunch. 2nd Scenario $\Omega = 1$ A flat Universe- it stays as it is. 3rd Scenario $\Omega < 1$ - it is open Universe. It expands to cold death. 4th Scenario- $\Omega = 1$ with inflationary phase. Its end may be a bouncing Universe.

3. The First Proposal of Inflationary Phase Preceding the Sedately Expanding Universe

Albert Einstein in 1915 set up the field equation for our Universe based on General Relativity Theory (GRT). He had an expanding Universe as the solution which he thought was untenable and hence he added an arbitrary constant to make it static.

After the publication, abbe Georges Lemaitre (Belgium), Willem de Sitter (Holland), Alexander Friedmann (Russia) gave

different solutions to GRT field equations. Out of these De Sitter solution was nearest to the inflationary model. Lemaitre started his Universe from a primeval atom. Friedmann Universe also expanded from a very dense clump of matter but with no cosmological constant. These could explain the sedately expanding Universe but how the pop up Universe from a Metaverse Cosmos could sustain as an independent Universe remained unanswered.

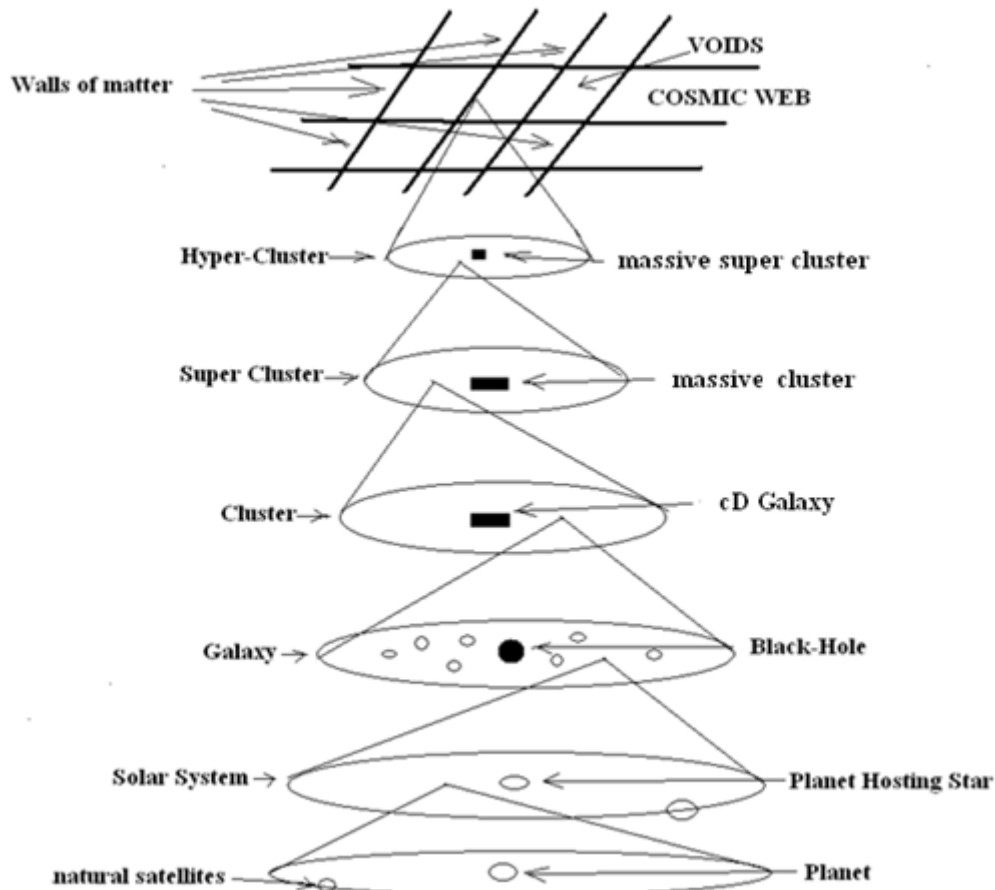


Figure 31. Dark Matter built the scaffolding of CORMIC WEB on which the Baryonic Matter clumped to form top-down hierarchy from hyper-cluster to super-cluster to cluster to galaxy to solar systyems to planetary systems with natural saellites.

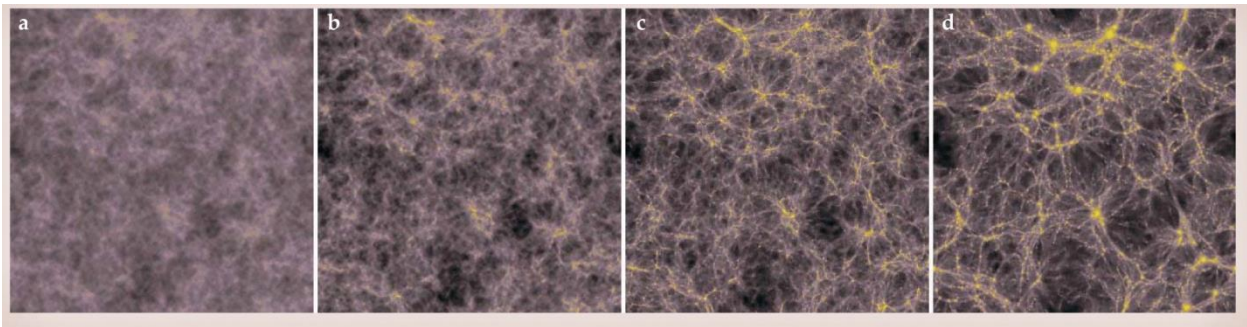
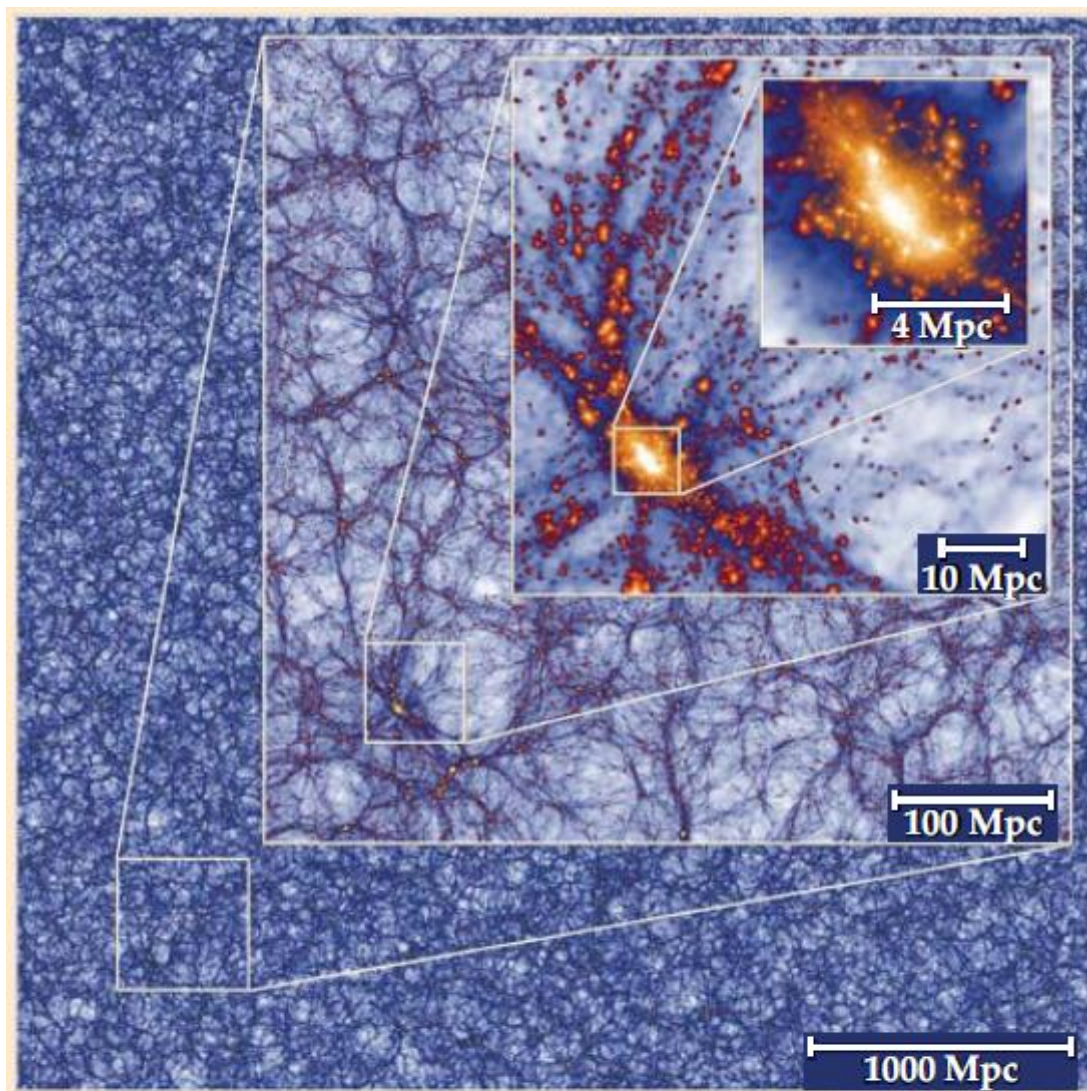
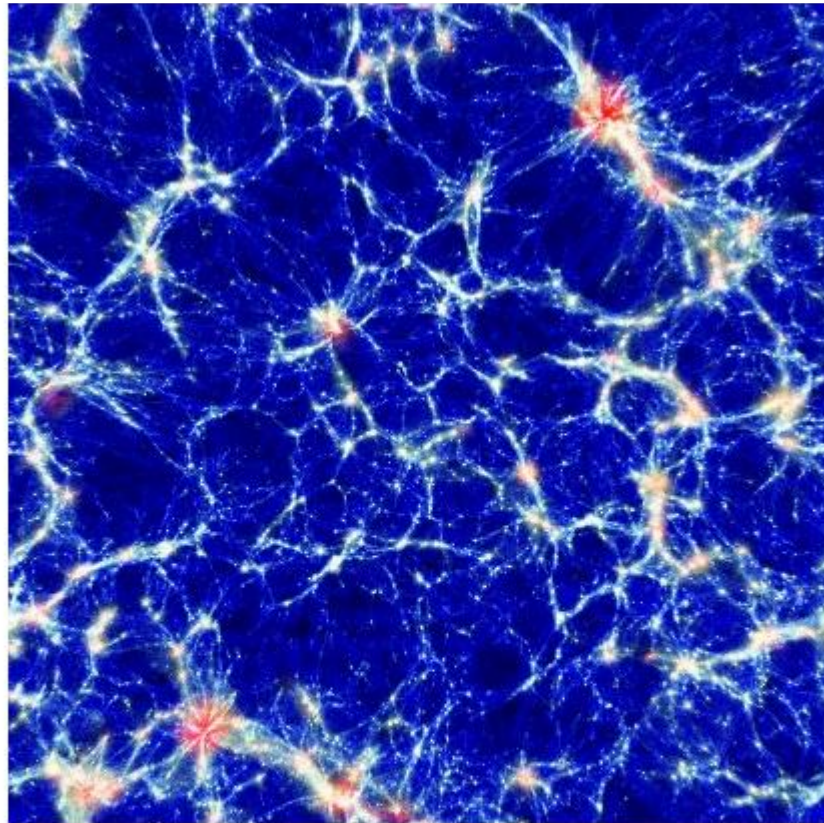


Figure X [Fractal95.eps] Computer simulation of the ever-increasing clustering of matter (dark plus baryonic) due to gravity in the post-plasma universe. Despite the overall Hubble expansion, initial low-contrast density perturbations (a) become more pronounced as overdense regions attract matter away from underdense regions. The result in recent times (d) is structures such as superclusters of galaxies and voids that extend over hundreds of millions of light-years. Yellow indicates regions of highest density. [Citation: Phys. Today 61, 4, 44 (2008); <http://dx.doi.org/10.1063/1.2911177>]



The cosmic web. Dark-matter distribution in a slice of 8 megaparsecs predicted from the Millennium XXL simulation within a box of 4.1-Gpc side length. At present, this simulation is the largest of its kind, with more than 300 billion particles. (Courtesy of Raul Angulo, Volker Springel, and Simon White; see also ref. 3.)

Figure 28. Fractal 67. The Cosmic Web at varying Zoom-in levels. It clearly shows, in the inset of 10Mpc, the formation of a cluster at the intersection of the filamentary network.



Numerical Simulation of the Cosmic Web. This shows how matter in our Universe is arranged on a very large scale forming a wispy network of clusters, filaments and voids known as Cosmic Web. Clusters form at the densest knot in this network where filament intersect. This image a portion of the cosmic web which spans 900Mly. The spacing of the filaments are less than 500Mly and hence they could be a result of the overlapping of BAO emnating from the hot spots in CMBR image.

Figure 5. Fractal 62. Numerical Simulation of the Cosmic Web

Date: 20 Nov 2012

Satellite: Planck

Depicts: Numerical simulation of the cosmic web

Copyright: Image courtesy of Klaus Dolag, Universitäts-Sternwarte München, Ludwig-Maximilians-Universität München, Germany

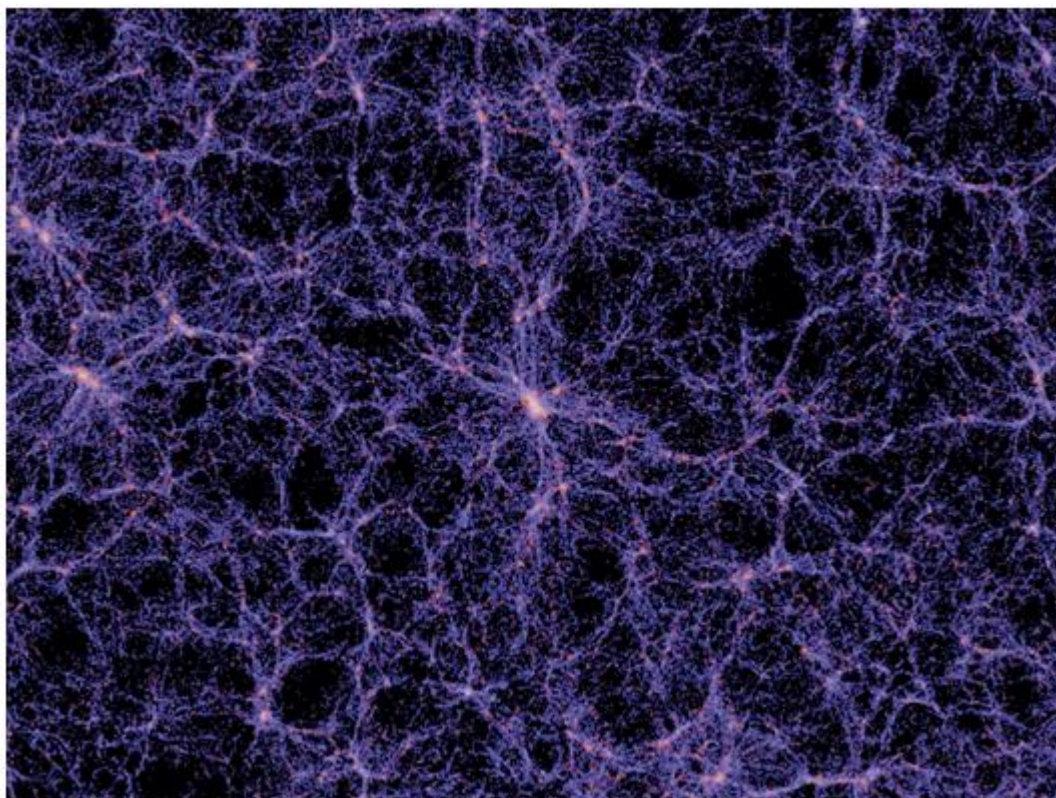


Figure 3. Fractal 2.Large Scale Distribution of Baryonic Matter as evidenced by large scale light distribution. [Curtsey-Large Numerical Simulation for Dark Energy Surveys@Marenostrum Supercomputer]

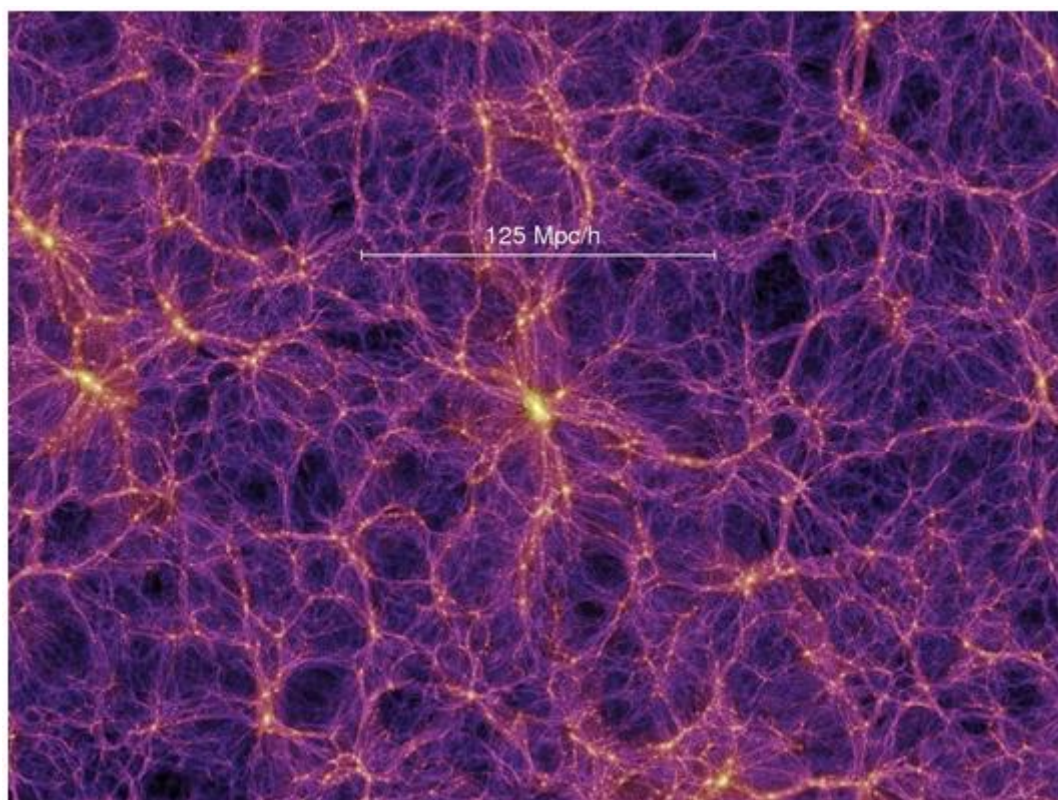


Figure 4. Fractal 3. Large Scale Distribution of Dark Matter. [Curtsey-Large Numerical Simulation for Dark Energy Surveys@Marenostrum Supercomputer]

In 1944 George Gamow along with Ralph Alpher and Robert Herman came up with a comprehensive theory of expanding Universe from primordial state. This was called the Big-Bang theory. Their theory predicted 3K black body relic radiation in our present Universe left over as a legacy from the Big-Bang. This is called Cosmic Microwave Background Radiation (CMBR) which was subsequently discovered by Wilson and Panzias in 1965 while testing their microwave horn antenna for Radio Astronomy. For this 1978 Physics Nobel Prize was rewarded to them. But even this could not explain the beginning or the kick start process for Big-Bang because as already mentioned a hot (1032K) and (1094gm/cc) dense compact object is doomed to be entombed in a black hole right at the beginning.

Inflationary phase of exponentially expanding Universe had to be incorporated in Big-Bang Model. Exponential expansion is faster than light. The matter inside the Universe fabric is not travelling at velocity faster than light but in fact matter and energy are frozen in the original uniformity of the primordial quantum bubbles. Starobinsky Model was the first model incorporating inflation in 1970. Alan Guth of MIT independently proposed a similar model in 1981. This was improved upon by Andrei Linde and is called the New Inflation Model.

4. Reconciliation between the Observed Universe and Expanding Universe Model

Allan Guth postulated inflationary phase of expansion or exponential phase of expansion in the first split second before it was launched on a decelerating expansion phase. To achieve an ultimate cosmic free lunch a kick-start had to be given before a decelerated expanding Universe could be sustained as shown in the Figure 18 Fractal 94.

In a metaverse devoid of everything, several universes were popping up and they could have very well collapsed as suddenly had these several universes not received kick starts to sustain as independent expanding Universe. Each pop up was a BB and

sum total of gravitational energy plus matter energy was zero. Here we take help of particle physics to explain this kick start which sustained the expanding pop universes.

5. Back to Standard Particle Physics and Grand Unified Theory (GUT)

In early Universe we were in Planck's era. As given in Table 2, quantum bubble was at 10^{32}K temperature equivalent to $(k \times T/e = 10^{19}\text{GeV})$. Time after the pop up of quantum bubble was 10-44s. Dimension of the bubble was 10^{-33}cm , mass of radiation was $10^{19}\text{GeV}/c^2 = 10^{-5}\text{gm}$ and super density was 10^{94}gm/cc . There was only radiation present.

At Planck's time 10-44s, Gravity as a fundamental force separates from Grand Unified Force of strong+electroweak. At GUT scale time of 10^{-35}s , Strong force (Quantum Chromodynamics) separates from electro-weak force. There is a phase transition and spontaneous symmetry breaking just as it happens when water freezes to ice. Rotational symmetry is broken and latent heat of phase transition is released. There are topological defects as we have domain interfaces in ice cube. Because of this GUT phase transition a large number of magnetic monopoles are produced which are the point topological defects but we don't find any magnetic monopole in the present time.

QCD and Electroweak force together make the Standard Model. In standard model we have SU(1), SU(2) and SU(3). SU(3) takes care of QCD and SU(1) and SU(2) take care of electro-weak force.

Above 10^{14} GeV to 10^{15} GeV , strong and electroweak are unified but at energy lower than 10^{14} GeV they split into strong and electroweak by spontaneous symmetry breaking. In 1974, GUTS was introduced which combined the standard model with gravity. In 1974 minimal SU(5) was proposed. GUT gives the symmetry between electron and quark. This is the reason why the magnitude of charge of electron and proton are exactly equal.

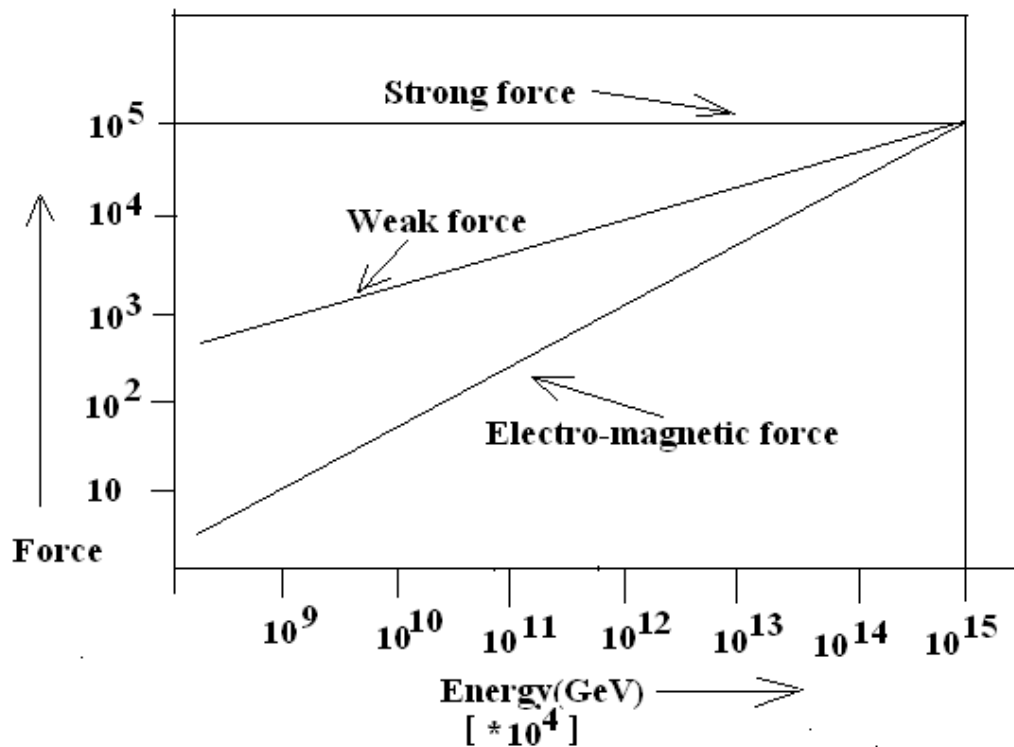


Figure F.1 Comparative plot of Strong, Weak and Electro-magnetic forces.

Symbol	Parameter	Magnitude
M_{pl}	Planck Mass	$1.2 \times 10^{19} \text{ GeV}/c^2$
L_{pl}	Planck Length	$1.6 \times 10^{-33} \text{ cm}$
t_{pl}	Planck Time	$5.4 \times 10^{-44} \text{ sec}$
T_{pl}	Planck Temperature	$1.4 \times 10^{32} \text{ K}$
We start from Planck's era for our analysis. Laws of Physics hold good till this limit		

Table 2. mass, length, time and temperature in Planck Era

Characterization	Forces Unified	Time from start	Energy(GeV)	Temp(K)
All 4 unified	All 4	0	∞	∞
Gravity separates	Strong+Weak+EM	$t_{pl} = 10^{-43} \text{ s}$	10^{19} GeV	1.2×10^{32}
Strong Force separates	Weak+EM	10^{-35} s	10^{14} GeV	1.2×10^{27}
Electro-weak split	None	10^{-11} s	100 GeV	1.2×10^{15}
Present	None	10^{10} y	10^{-12} GeV	12

Table 3. Unification points of the four fundamental forces

Gravity splits from GUF(grand unified force) at 10^{-43} s at 10^{19} GeV by spontaneous symmetry breaking leaving behind relic gravitons. Not much is known of this era.
Strong Nuclear Force separates from Electro-weak unified force at 10^{-35} s at 10^{14} GeV by another spontaneous symmetry breaking

leaving behind relic quarks and magnetic monopoles as point topological defects.

As Universe cools, further phase transitions occur and matter + radiation evolves as given in Table 4.

Time	Temp.	Epoch	Description	Comments
10^{-43} s	10^{32} K	Planck's	Gravity Force separated	Strong+Electroweak Unified
10^{-36} s	10^{28} K	GUT	Grand unification era	
10^{-35} s	10^{27} K	Inflationary Phase	Strong force splits off	Strong Force Splitting triggers Inflationary phase
10^{-32} s	10^{22} K	Inflationary Phase ends	Universe settles from false to true vacuum	Inflates from 10^{-33} cm to 5cm size
10^{-12} s	10^{16} K	Quark epoch		
10^{-6} s	10^{13} K	Quark epoch ends Hadron epoch begins	Quarks are confined to baryons and bosons	Baryon number will be conserved
10^{-4} s		Neutrino generated		
1s	10^{10} K	Lepton Epoch Neutrino decouples from plasma	$e + \text{anti } e = \text{photon} + \text{photon}$	Universe becomes transparent to neutrino
3min	745K	Lepton epoch ends Nucleosynthesis begins	$\text{Photon} + \text{Photon} = e + \text{anti } e$	
20 mins	289K	Nuclosynrthesis ends	H nuclei and He nuclei stabilize but in plasma 92% H nuclei+8%He-nuclei	Radiation dominated era Photons interact plasma
60,000y			DM decouples and starts building COSMIC WEB	
240,000y	3633K	Recombination & radiation starts		
400,000y	3250K	decoupling	75%H+25%He by mass stabilizes	Transparent Universe surrounded by CMBR
245My		1 st generation starts emerging	2 nd reioniztion and dark ages end.	
1.1by		Half reionization complete		
3.2754by		Cosmic high noon		
8.9by		Cosmic jerk		
	4.567bya	Sun formed		
	4.467bya	Earth fully formed and Moon born by Giant Impact		
	3bya	Bacterial life is born		
	700Mya	Primitive animals		
	540Mya	Pre-cambrian explosion		
	200Mya	Mammals evolve		
	65Mya	Dinosars become extinct		
	600,000ya	Homosapiens society		
	170,000ya	In LMC, 1987A undergoes Core Collapse.	Its neutrinos are detected first in UCI on the evening of 23 rd Feb 1987	After neutrinos the light from SN explosion reach Earth abnd detected by Ian Shelton.

Table 4. Timeline of Evolving Universe from first Pop-Up

6. Physics of Inflationary Phase

At time = 10^{-36} s and temperature 10^{28} K, there is one unified Strong and electroweak force.

At time = 10^{-35} s and temperature 10^{27} K,, strong force separates and there is spontaneous symmetry breaking and phase transition. This results in topological point defects in form of Magnetic Monopoles. Latent heat is released.

At time = 10^{-33} s and below 10^{27} K, SU(1), SU(2), SU(3), acquire separate identities.

The anticipated spontaneous symmetry breaking can be immediate or it can be delayed. If it is immediate magnetic monopole will be produced in abundance and inflationary phase will not be triggered. Instead if it is delayed we say that Universe is super cooled and it is said to be in false vacuum state. This happens only at very high matter density of 10^{60} ×nuclear density.

In false vacuum, matter is in lowest possible density and that can be attained without spontaneous symmetry breaking. As false vacuum continues latest energy density is maintained constant even though universe is expanding. GRT combined with false vacuum produces a powerful repulsion which results in powerful kick-start of the inflationary phase. Eventually when energy density cannot be maintained constant and it falls, the spontaneous symmetry breaks and false vacuum decays and universe settles in real vacuum. False vacuum transfers all its energy to the inflated Universe which reheats and gets into a sedate expansionary mode.

While in false vacuum, Universe is doubling in size at time intervals of 10^{-34} sec and in a split of second of 10^{-32} sec through 112 doublings Universe inflates from 10^{-33} cm to 5cm- an enormous expansion.

This enormous exponential expansion in split of a second

$$\Omega = \frac{1}{10^{-6}t^2} \frac{gm}{cc}; \&T = \frac{10^{10}}{\sqrt{t(s)}} Kelvin; T^* = \frac{1}{\sqrt{t(s)}} MeV; R = 5 \times 10^2 (\sqrt{t}) cm; \quad (4)$$

This inflationary model has a general character: Standard Model plus three light fermionic singlets can simultaneously explain neutrino mass, cold dark matter, baryon asymmetry and inflation without invoking any new particle. This is known as γ MSM(Minimal Standard Model with three species of neutrino with total mass less than electro-weak scale).(Asaka & Shaposhnikov 2005; Asaka et.al. 2005).

simultaneously solves the flatness problem, horizon problem, magnetic monopole problem , photon abundance problem and energy density fluctuation problem in the early Universe.

In static Universe over-density growth is exponential but in inflationary scenario it is linear (Smoot. 1992). Within this scenario the Universe underwent a brief period of accelerated or exponential expansion (Starobinsky 1979, 1982; Kazanas 1980, Guth 1981, Sato 1981, Linde 1982, Albercht & Steinhardt 1982). During this accelerated inflationary phase, quantum fluctuations were inflated in scale to become the classical fluctuations that we see today in the CMBR image.

The sudden ballooning of the Universe also amplified quantum fluctuations in matter density into clumps of matter that went to seed the first star and eventually the straggly super-cluster of galaxies.

The wrenching moment of inflation should have shaken the space-time fabric resulting in strong Gravitational Wave radiations which should leave B-Mode polarization pattern on CMB image .

3. Chapter 3. End of Inflationary Phase

Inflationary phase lasted for Planck's time = 10^{-32} seconds. In this period Universe expanded doubling 112 times and it grew from 10^{-33} cm size to 5cm size. After Planck's time it expanded more sedately in decelerating fashion and as size grew temperature of our Universe fell.

During the monotonic phase of expansion, the matter density(gm/cc), temperature T in Kelvin and T* in MeV decrease and Hubble Radius increase according to the following power law(Schilling 2001):

4. Chapter 4. The Early Universe

Timeline of our Early Universe is given in Table 6. Exploration of the Early Universe will be facilitated by 30M Telescope and by the launch of James Webb Space Telescope in 2018.

z	Years after BB	Cosmic Event
Infinity	0	Big Bang occurred
3402	67,000	Dark Matter decouples from the energy field and experiences gravitational clustering.
1090	400,000	All gases neutralize and light absorbing haze plunges the Universe in Cosmic Dark Age.
1090 to 14	400000 to 300My	Cosmic Dark Age prevails.
≤ 14	300My onward	Non-linear growth of DM+BM leads to star formation.
14 to 10	300My to 500My	Universe is filled with faint small galaxies which are the dominant source for re-ionization of Inter Galactic Medium (IGM).Burst of star formation.
9.6 ± 0.2	$(490\pm 15)\text{My}$ -3.6% of Universe Age	By gravitational lensing, Zheng et.al (2012) detect the farthest cluster called MACSJ1149+2223. They also detect the abundance of faint Galaxies which are the dominant source of re-ionization.
10 to 6	500My to 1G	Re-ionization phase of IGM is completed.

Table 6. Timeline of the Cosmic Dawn(Stark 2012)

5. The First Evidence of the Evolving Universe (Pastorella & Patal 2008)

On Nov.11, 1572, Brahe was a witness to a brilliant new star in the constellation Cassiopeia. The star became as bright as Venus and could be seen for two weeks in broad daylight. After 16 months it disappeared. Brahe documented “unlike our Moon and the planets, the light’s position did not move in relation to the stars. That meant it lay far beyond the planets of our solar system”.

The contemporary view of the distant heavens was that it was perfect and unchanging. The birth of a new star and its subsequent disappearance came as a rude shock to the commonly held belief that the heavens were static.

6. The Detection of Novae, Supernovae and Dark Matter. (Heckman & Kaufmann 2011)

In 1933, Fritz Zwicky was working on COMA cluster of galaxies. There was too little visible matter to hold together the cluster together. The clusters seemed to be orbiting around a central massive core too fast. Four decades later this kind of missing mass was found in Galaxies also. So it was postulated that each galaxy is embedded in a vast clump of dark matter known as ‘halo’. Dark Matter is inferred from the gravitational effects and from the gravitational lensing of the Cosmic Microwave Background Radiation (CMBR).

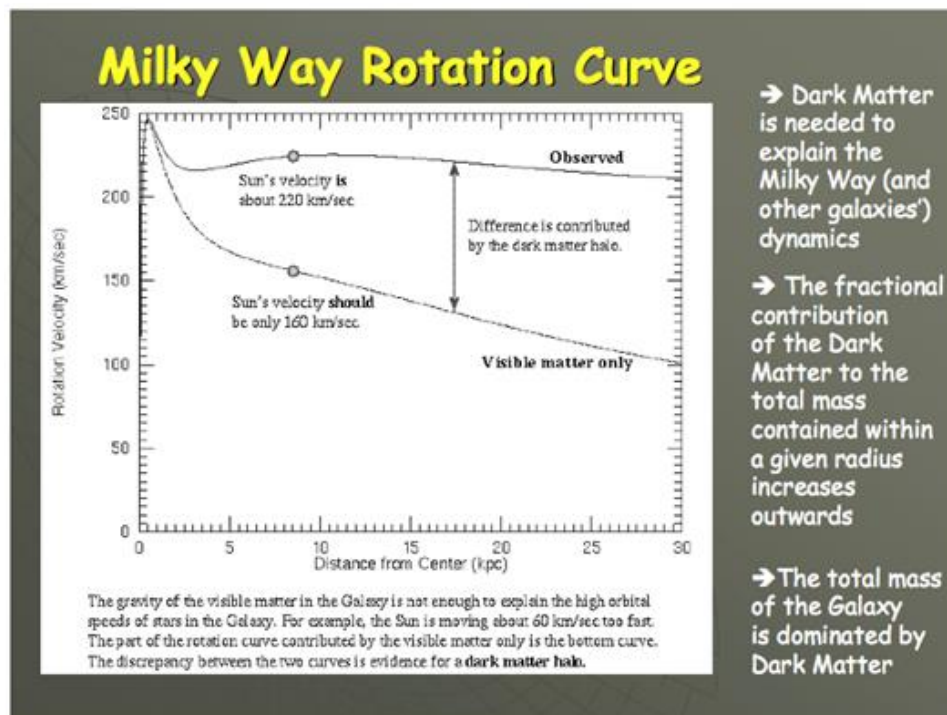


Figure 27. Fractal 5. Observed tangential velocity profile of the stars in Milky Way at increasing distance from the center of Milky Way and theoretically expected value based on the visible matter only.

In a work by Klypin, Anatoly et al (2003) it was shown that if the mass to luminosity ratio $Y_{\bullet} = M_{\odot}/L_{\odot}$ for Sun-like-Star then the mass to luminosity ratio for Galaxies and Clusters comes out to be $Y_{\bullet} = K.(M_{\odot}/L_{\odot})$ where $K = 2$ to 10 . For Local SuperCluster 'K' come out to be 300 and for Milky Way it comes out to be 2.7. This variation in 'K' is the clinching evidence in favour of the dark matter.

Wilkinson Microwave Anisotropy Probe (WMAP) measured Big Bang's after-glow "Cosmic Microwave Background Radiation". The temperature was found to vary even so slightly. The pattern of hot and cold spots reveal the heterogeneity at the age of 380,000 years after the Big Bang. This wee bit heterogeneity subsequently evolved in top-down model into super-clusters, clusters, galaxies and solar system and could explain the present large scale structures of the COSMIC WEB. Universe is constrained to have 4% ordinary matter, 23% dark matter and 73% dark energy, all interacting through gravity[SOM_Appendix F]. This dark matter can be explained in one of the following manners:

Super symmetry of matter predicts that Big Bang should leave right amount of WIMP after the Big Bang which will correctly account for the 23% of dark matter required for maintaining the Cosmic Web of the visible matter intact.

7. What is CMBR ?

Launch of COBE (Cosmic Background Explorer) started the era of precision measurement of the Cosmic Microwave Background(CMB) Radiation.

What is CMB ?

According to Big Bang theory, our Universe started from a singularity. It rapidly inflated to a very large size in time interval from 10^{-34} seconds to 10^{-32} seconds. Its event Horizon expanded faster than light speed. After 10^{-32} seconds, Universe expanded sedately and monotonically. (Schilling 2001)

Initially the four forces (Gravitational forces, Strong forces, Weak forces and Electro-magnetic forces) were of equal magnitude as a single Force as shown in Figure F.1.

From 0 second to 10^{-43} second, temperature fell from infinity to 10^{19} GeV, radius of the Universe expanded from 0 to 10^{-33} cm. Below 10^{19} GeV, super symmetry is broken and Universe makes a **phase transition from Quantum Gravitation to Grand Unified Phase**. *Gravitational force decoupled and relic Gravitons were left behind* which we should be able to measure but have not been able to measure till now.

From 10^{-34} sec to 10^{-32} sec, Universe experienced an inflationary expansion. The event horizon surrounding the singularity expanded at a speed greater than the speed of light.

At 10^{-33} sec, **phase transition from Grand Unified Phase to Electro-weak phase** took place. Strong force splitted from electro-weak force. This Spontaneous Symmetry Breaking. The Latent heat of Phase Transition is released which gives the kick start to the pop up Universe

By 10^{-32} sec, Universe expanded from a singularity of zero dimensions (10^{-33} cm) to a base ball size sphere (5cm). After this, Universe expanded sedately and monotonically and in decelerated fashion as shown in Figure 18 (Fractal 94.eps). The inflationary phase was over.

At 10^{-12} sec, temperature fell to 10^{15} K and energy fell below 100GeV. *Weak force decouples and relic Intermediate Vector Bosons W^+ , W^- and Z^0 are left behind*. Below 100GeV, weak forces and electro-magnetic forces are separated. This phase transition is also known as Salam-Weinberg Transition in honour of Abdus Salam and Steven Weinberg who worked out the electro-weak theory.

At 10^{-6} sec, temperature fell to 1GeV. Below 1 GeV, there is **Quark-Nucleon Phase transition**. *Strong forces get decoupled, quarks are confined to baryons (which are triplets of quarks) and mesons (which are doublets) and relic quarks are left behind*. Baryons are the nuclear particles like protons and neutrons and mesons mediate the strong force within a nucleon. In this decoupling residual quarks are left behind as relic quarks which should be detected with its abundance as high as that of gold but till date no relic quark has been detected.

At 1s, neutrinos decouple from the quark-baryon plasma and create Cosmic Neutrino Background (CNB) which we today see at 1.9K. Creation-annihilation stops and feeble remnant of matter is left over because of baryon asymmetry. And n:p ratio shifts from 50:50 to 25:75.

At $t = 100$ s, He Nuclei formed along with H nuclei. At 3mins(180s), temperature is low enough for stable light nuclei and n:p ratio is 13:87 and we have 75%H₂+25%He. There is a plasma of nucleons and leptons. Atoms cannot form.

At 67000 years, DM decouples and starts building the scaffolding on which the cosmic web will be interwoven. At 370,000 years after the Big-Bang the temperature of the hot soup known as plasma, the fourth state of matter, consisting of proton, neutrons and electrons falls to 4000K. Below 4000K, plasma gets neutralized into a neutral gaseous mixture of H₂ and He. Radiation decouples leaving behind relic photons. Today after 13.8Gy, these Relic Photons have cooled to 2.7K Black Body Radiation. This 2.7K Black Body Radiation is known as Cosmic Microwave Background Radiation(CMB radiation).

For 370,000years after the Big Bang, matter was in a plasma state and through Compton Scattering, matter and photon were kept in thermal equilibrium though they had different adiabatic indices. Because of Compton Scattering, photons had the same density distribution as the matter density distribution. When temperature fell below 4000K, matter and radiation got decoupled and matter changed from ionized state to neutral state. Since the two cooled independently, Temperature of matter fell inversely as the square of the Radius of the Universe and temperature of radiation fell inversely as the Radius of the Universe. But the Black body Radiation carried the imprint of the matter density distribution at the time of parting at 370,000 years after the Big Bang.

Subsequently after the decoupling matter has evolved as a very differentiated and non-homogeneous system of super-clusters, clusters, galaxies and as exo-solar systems. If today we have such a non-uniformity of matter distribution then at 370,000 years after the Big Bang, we should have the seeds of this non-uniformity and this imprint should be present as hot and cold

spots in CMB radiation. The imprint of BAO ripples should also be present as metric scale.

In 1960's AT & T, Bell Lab used a radiometer in a telescope that would track the early communication satellites namely Echo-1 and Telstar. This radiometer was being tested by Arno A. Penzias and Robert W. Wilson. In course of this testing they detected a background noise in microwave spectrum. It corresponded to 2.776K Cosmic Microwave Background Radiation(CMBR). As shown in Figure Fractal 68 They were led to this idea by the news that Robert H. Dicke had suggested in 1940 that a radiometer would detect this CMBR.

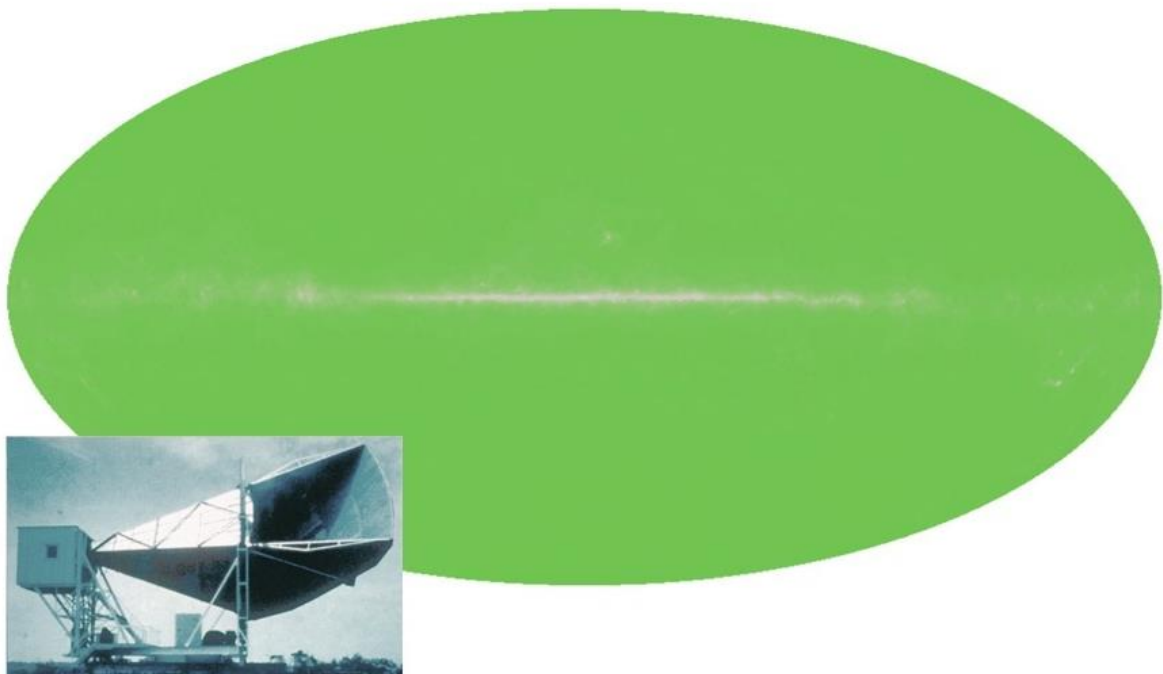
The discovery firmly established the Big Bang Theory. In 1978 the Nobel Prize in Physics was awarded to Arno A Penzias (American), Robert Woodrow Wilson (American) and P.L. Kapitza (Russian) for the discovery of Cosmic Microwave Background Radiation.

7.1 COBE

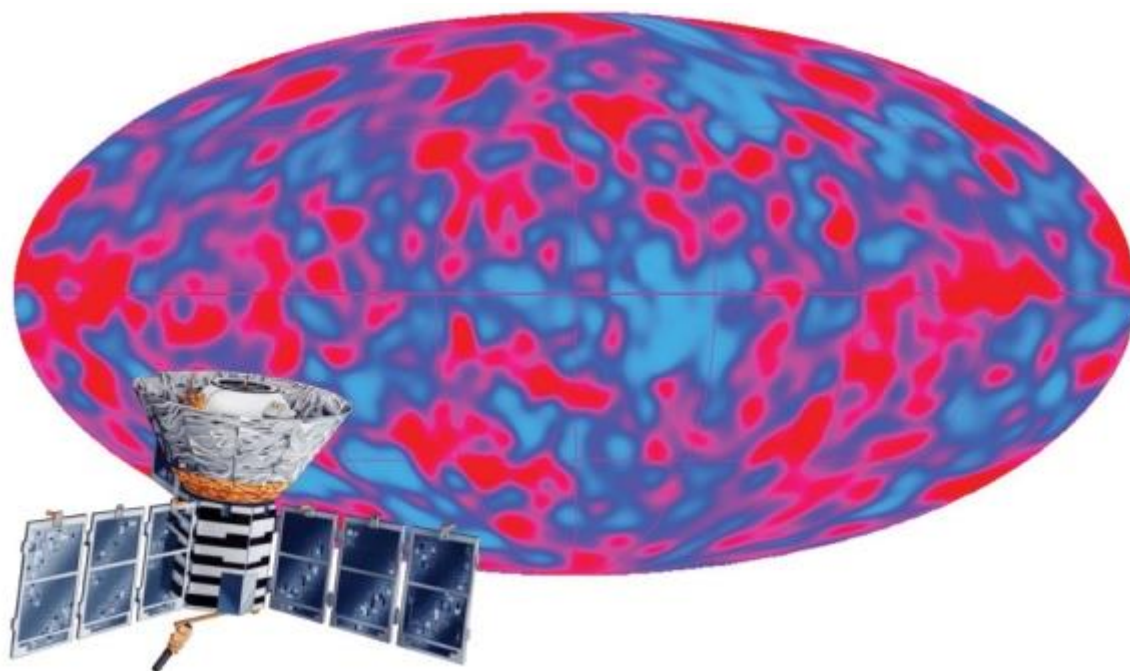
In 1990, a satellite called COBE (Cosmic Background Explorer) measured the spectrum and temperature variations in the background radiation pattern. The spectrum was exactly as expected for 2.7K Black Body radiator. The temperature variation was 1 in 100,000 as seen in Fractal 69. Till then CMB radiation had appeared as perfectly isotropic and isotropic radiation pattern cannot explain the galaxies, clusters and super-clusters formation. Therefore the achievement of COBE marked the correctness of the Big Bang Theory.

7.2 WMAP

To refine the CMB radiation pattern studies, in 2001 Wilkinson Microwave Anisotropy Probe was launched (WMAP). This is in a circular orbit around Sun with semi-major axis $a = + 1.5 \times 10^6$ km.



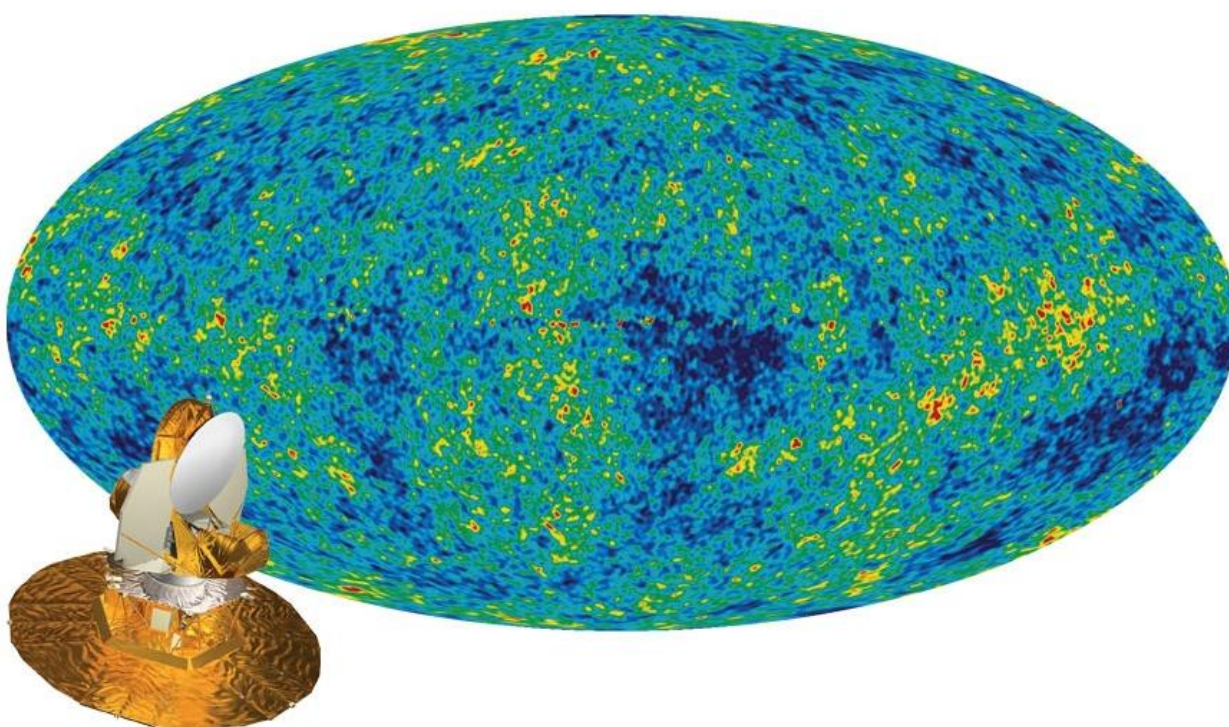
Fractal 68. In 1965, Arno Penzias and Robert Wilson discovered the cosmic microwave background. Their giant but crude microwave receiver saw the radiation as being the same in all directions, occurring at 2.7 kelvin.



Fractal 69. It was not until the launch of the Cosmic Background Explorer (COBE) spacecraft that astronomers could begin to see variations in the background, at levels of 1 part in 100,000.NASA.

In February 2003, the image of the infant cosmos only 380,000yrs old was received. The results from WMAP reveal that the CMB temperature variations follow a distinctive pattern predicted by

cosmological theory: the hot and cold spots fall in characteristic sizes .The image of infant cosmos is shown in Figure Fractal 70.



Fractal 70. The Wilkinson Microwave Anisotropy Probe, launched in 2001, improved on COBE by looking for such anisotropy at much smaller angular scales.

The hot spots or the red spots in CMB image are the images of compressed, dense plasma region and cold spots or the blue spots in CMB are the signature of rarefied plasma. The red spots are the primordial fluctuations which gave rise to dwarf galaxies

in Early Universe. These dwarf galaxies through hierarchical clustering gave rise to clusters and superclusters based on Cold Dark Matter(CDM) Bottom-Up Model. Out-of-equilibrium CDM material condense to small density fluctuations seen

as red-spots in CMB image. Dark Matter haloes collect the plasma in sonically oscillating gravitational potential wells. These hierarchically cluster to form larger and larger CDM haloes. These CDM haloes and their interconnections form the scaffolding around which the small scale, intermediate scale and large scale Universe evolve starting from stars to galaxies to clusters to super-clusters. N-body computation of the clustering of materials in a Universe dominated by CDM results into the characteristic pattern of sheets, filaments and knots as observed in Large Scale Universe. But on intermediate and small scale that is less than 1Mpc baryonic matter becomes the dominant factor and hydrodynamic instability, core accretion, gravitational radiation and tidal heating comes into play in the evolution of Galaxies, Solar Systems and Planetary Systems. A simple Λ CDM cosmological model described by 6 parameters is an excellent fit to the five-year Wilkinson Microwave Anisotropy Probe (WMAP) temperature and polarization data (Dunkley et.al. 2009).

In July 2003, Scientists superimposed SDSS data on the microwave intensity map developed by WMAP. They conclusively proved that there is what is known as integrated Sachs-Wolfe effect. Clustering of galaxies cause dimple in space- time fabric. Anti- gravity outward push tends to stretch out the dimples in an otherwise flat Universe and in the process tends to crush the Cosmic Microwave Background Radiation at and near the dimples meaning by anti-gravity push shifts the microwave radiation towards shorter wavelength. This precisely was observed in the superimposed map. This is a definitive proof of dark energy dominance in our present Large Scale Universe.

The results from WMAP have been corroborated by SLOAN Digital Sky Survey(SDSS) and by Supernovae Cosmology Project (Seife 2003, Goldhaber & Perlmutter 1998) and they are the following:

- i. There is 4% ordinary Baryonic matter, 23% dark matter composed of exotic particles and 73% dark energy;
- ii. The Hubble Constant has been nailed at $H_0 = \text{Rate of expansion of our Universe} = 71 \text{ Km}/(\text{sec-Mpc})$;
- iii. The age of our Universe is fixed at 13.7Gy;
- iv. Supernovae Cosmology Project is consistent with Flat

Universe with Cosmology Constant being non-zero and positive. The result that there is 4% Baryonic Matter and 23% Dark Matter tells us that :

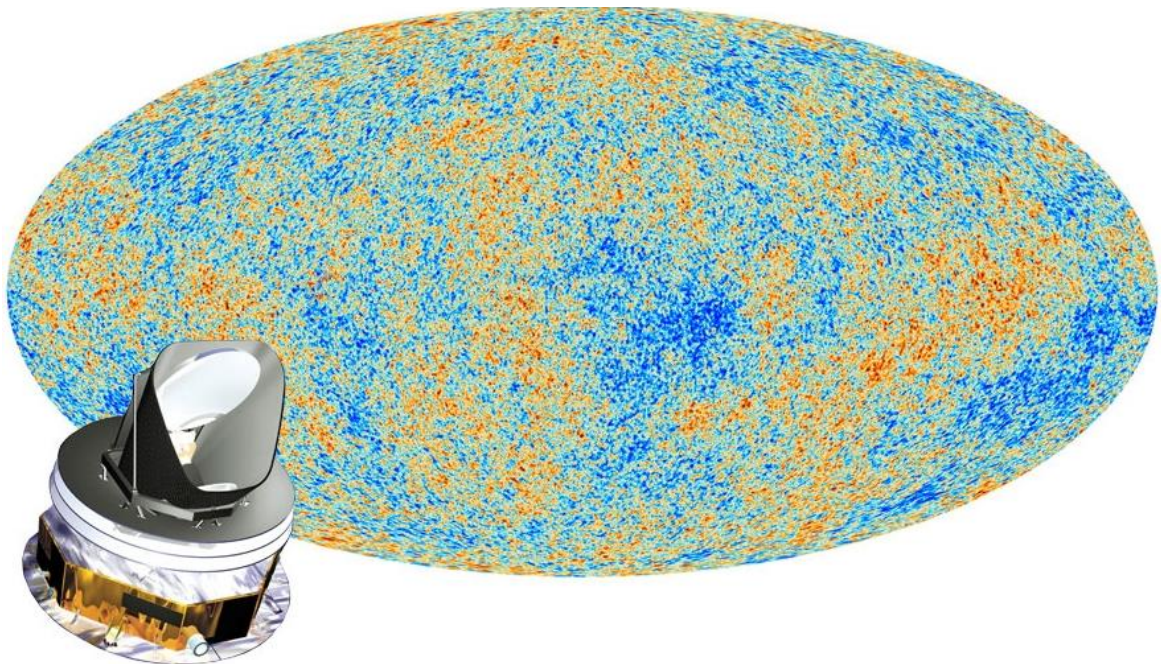
ordinary matter: dark matter $\equiv 1 : 5$ on an average in the Universe.

7.3 PLANCK Satellite was Launched to Further Refine the CMBR Data the CMBR data

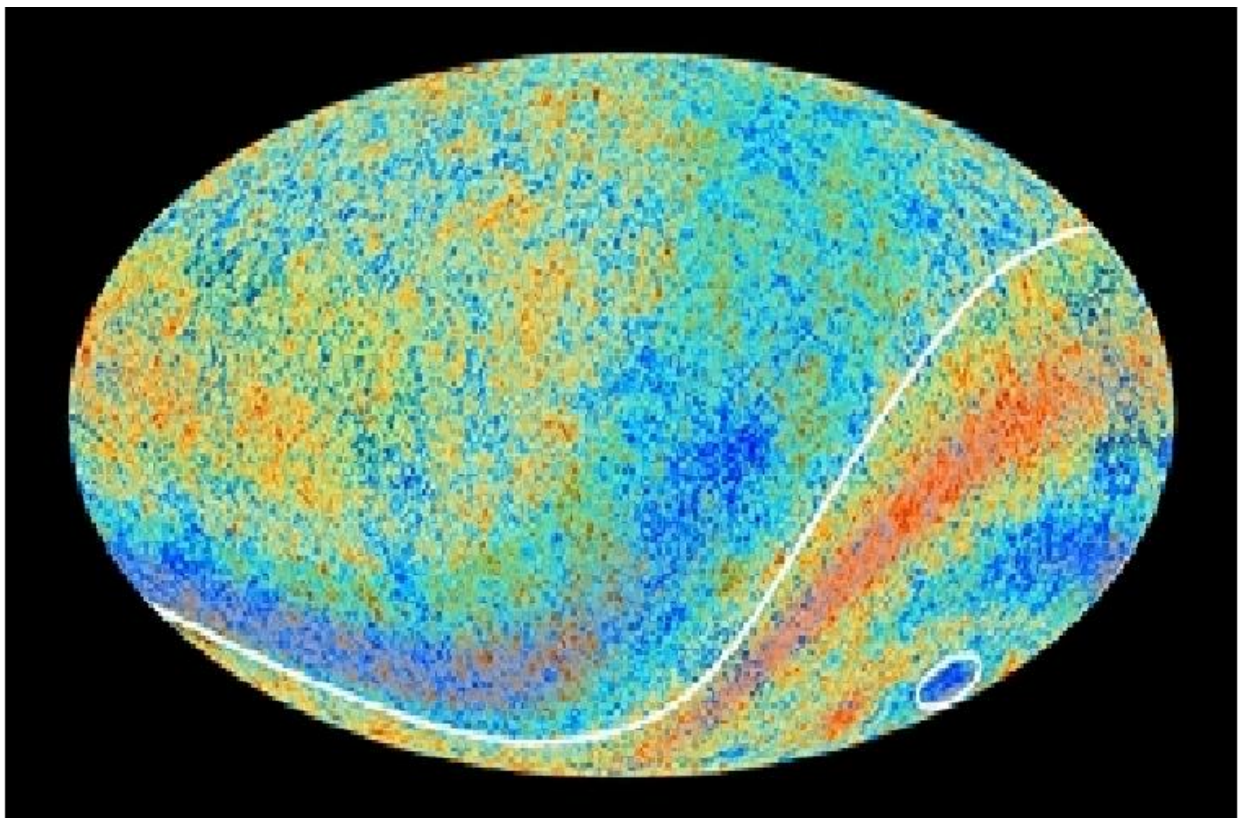
The Universe is not uniform on the largest scale as expected. Previous works had hinted that N & S Hemispheres of the sky donot look like each other (statistically speaking) as they should and that there is an anomalous cold-spot in the CMB(anomalous in terms of shape, not in terms of temperature or overall size). Planck supported these results of WMAP. Furthermore six parameters are slightly different for each half of the sky separately. If these effects are real they may hint at unpredicted structure that is larger than our Cosmic Horizon and originating before BB. Wiggly Power Spectrum fit remarkably well at small angular scales but temperature fluctuations at largest scale do not behave as well. The asymmetry defines a preferred direction in space. This points to the possibility of new physics of multi-Universe. The asymmetry in CMBR map hint that our Universe was born as bubble in a large Metaverse. The BB was sparked when Quantum Fluctuations in the Metaverse caused an excited Vacuum or false Vacuum in form of a new Universe to pop into being like an air-bubble in boiling water. The excess energy was derived from the surrounding Metaverse hence the new Universe sat on the bottom of an energy valley as shown in Figure 3[Fractal89.eps] and the new Universe had a saddle shape. Liddle et.al (2013) proposal of Open Universe inflation models, which are motivated by the string landscape and which can excite 'super-curvature' perturbation modes, can explain the presence of a very-large-scale perturbation that leads to a dipole modulation of the power spectrum measured by a typical observer and this explains the asymmetry observed in power spectrum of CMB map as first hinted by WMAP results and later supported by Planck results .

Planck's results are:

Baryonic Matter:Dark Matter:Dark Energy = 4.9% : 26.8% : 68.3%.



Fractal 71. Planck, launched in 2009, provides a capstone to the study of the cosmic microwave background. But unambiguous confirmation of a cosmic burst of expansion known as inflation remains elusive. ESA



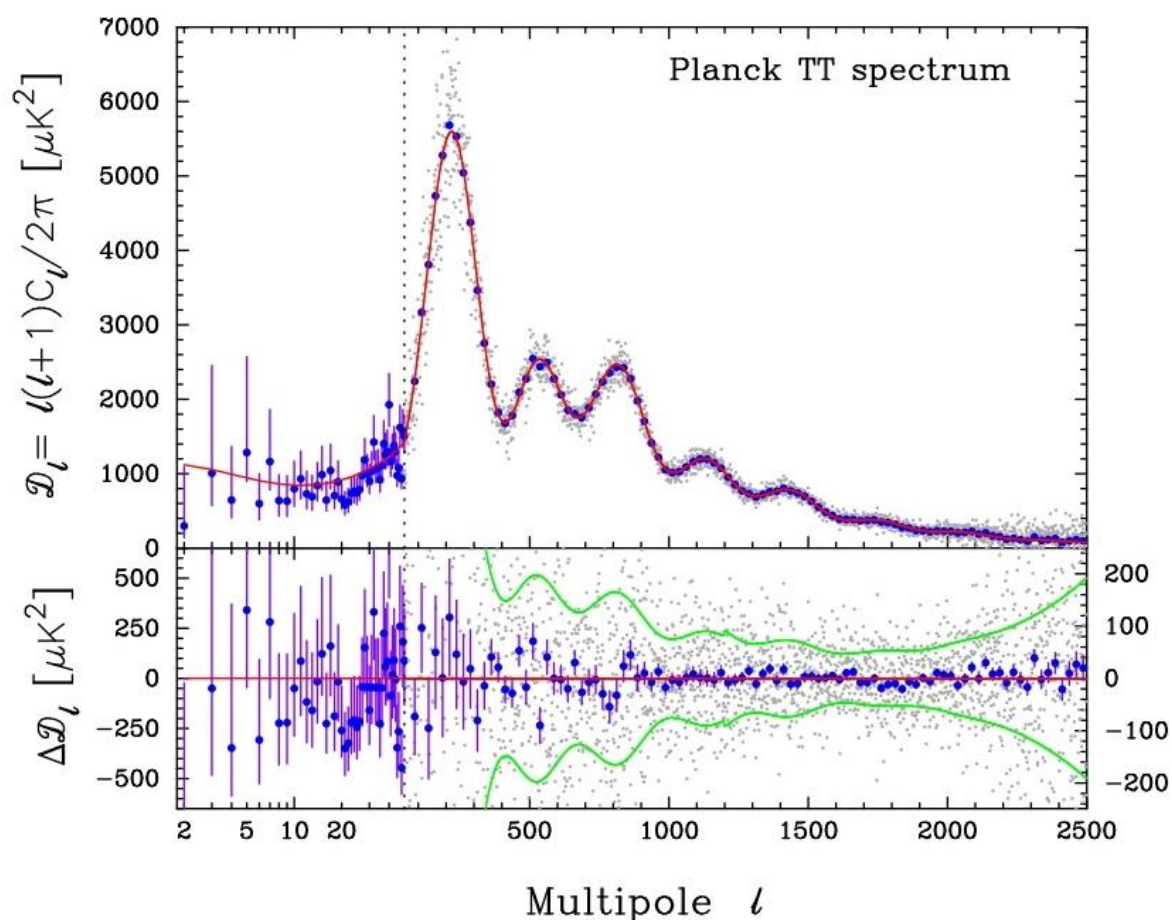
Fractal 72. Two Cosmic Microwave Background anomalous features hinted at by Planck's predecessor, NASA's Wilkinson Microwave Anisotropy Probe (WMAP), are confirmed in the new high precision data from Planck. One is an asymmetry in the average temperatures on opposite hemispheres of the sky (indicated by the curved line), with slightly higher average temperatures in the southern ecliptic hemisphere and slightly lower average temperatures in the northern ecliptic hemisphere. This runs counter to the prediction made by the standard model that the Universe should be broadly similar in any direction we look. There is also a cold spot that extends over a patch of sky that is much larger than expected (circled). In this image the anomalous regions have been enhanced with red and blue shading to make them more clearly visible.

On March 21st, 2013, scientists with the European Space Agency's Planck mission announced their long-anticipated results from the spacecraft's first 15.5 months of mapping the cosmic microwave background.

The CMB is the radiation released about 380,000 years after the Big Bang, when the newborn universe cooled down enough to become transparent and let light travel free. We see this light today redshifted to microwave wavelengths, wallpapering the whole sky behind the farthest galaxies. Slight temperature variations all across it reveal how matter was distributed at that early era. These variations allow cosmologists to test theories of what was happening in the universe in the tiniest instants after its birth, including how inflation drove the first 10^{-35} second of the Big Bang.

Planck's superbly precise new picture of the CMB (below) shows remarkable agreement with theoretical work, confirming that observations fit a simple cosmological model defined by just six numbers(parameters). (Take that in for a moment: the whole physical universe is described by six numbers(parameters). Even your phone number takes 10 digits in the U.S.)

The graph Fractal 74 shows how much temperatures fluctuate in patches of various angular sizes all across the sky. Our inflationary model makes specific predictions about what this complex graph should look like. As you can see, Planck's observations (red dots) trace nigh perfectly the theory (green line). My colleague Alan freaked out when he saw the tight fit at the graph's far right — you don't appreciate the wonders of scientific progress until you have a 6-foot-3 man jumping up and down in your office.



Fractal 74. Image Credit: Planck Collaboration: P. A. R. Ade et al., 2013, A&A Preprint

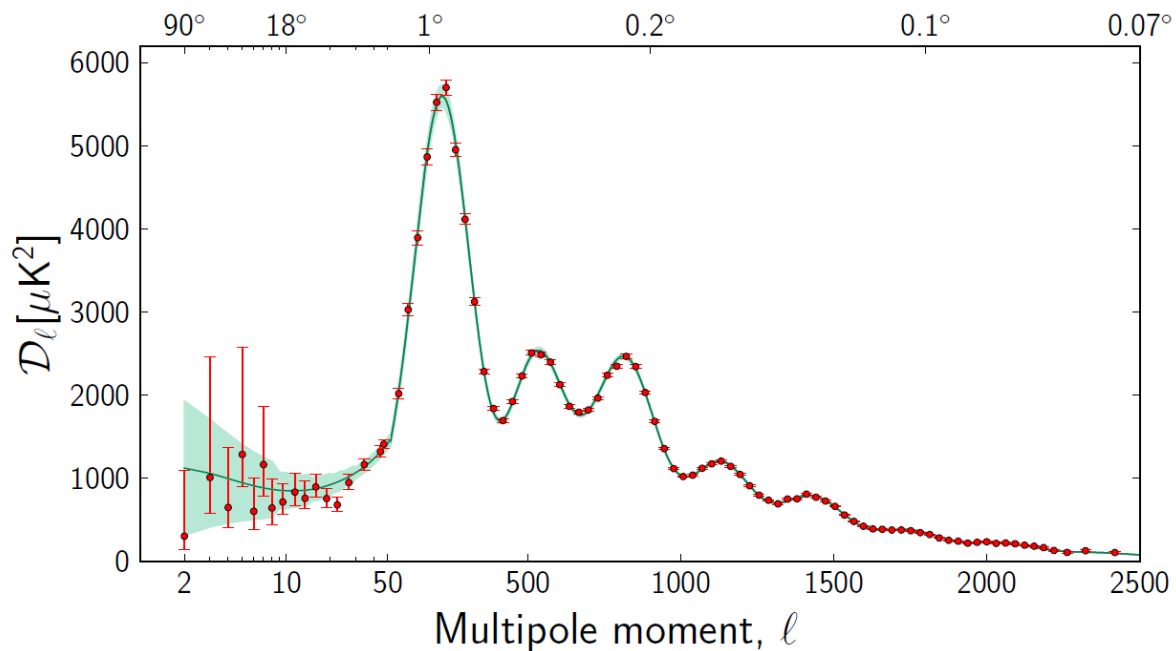
Planck foreground-subtracted temperature power spectrum (with foreground and other “nuisance” parameters fixed to their best-fit values for the base Λ CDM model). The power spectrum at low multipoles ($l = 2-49$, plotted on a logarithmic multipole scale) is determined by the Commander algorithm applied to the Planck maps in the frequency range 30–353 GHz over 91% of the sky. This is used to construct a low-multipole temperature likelihood using a Blackwell-Rao estimator, as described in Planck Collaboration XV (2013). The asymmetric error bars show 68% confidence limits and include the contribution from uncertainties in foreground subtraction. At multipoles $50 \leq l \leq$

2500 (plotted on a linear multipole scale) we show the best-fit CMB spectrum computed from the CamSpec likelihood (see Planck Collaboration XV 2013) after removal of unresolved foreground components.

The light grey points show the power spectrum multipole-by-multipole. The blue points show averages in bands of width $\Delta l \approx 31$ together with 1σ errors computed from the diagonal components of the band-averaged covariance matrix (which includes contributions from beam and foreground uncertainties). The red line shows the temperature spectrum for the best-fit base

Λ CDM cosmology. The lower panel shows the power spectrum residuals with respect to this theoretical model. The green lines show the $\pm 1\sigma$ errors on the individual power spectrum estimates

at high multipoles computed from the CamSpec covariance matrix. Note the change in vertical scale in the lower panel at $l = 50$.



Fractal 75. The temperature angular power spectrum of the primary CMB from Planck, showing a precise measurement of seven acoustic peaks, that are well fit by a simple six-parameter Λ CDM theoretical model (the model plotted is the one labelled [Planck+WP+highL] in Planck Collaboration XVI (2013)). The shaded area around the best-fit curve represents cosmic variance, including the sky cut used. The error bars on individual points also include cosmic variance. The horizontal axis is logarithmic up to $l = 50$, and linear beyond. The vertical scale is $l(l+1)Cl_{2-}$. The measured spectrum shown here is exactly the same as the one shown in Fig. 1 of Planck Collaboration XVI (2013), but it has been rebinned to show better the low- l region.

Planck launched on May 14, 2009, as successor to NASA's phenomenal Wilkinson Microwave Anisotropy Probe (WMAP), which mapped the CMB for nine years. WMAP observed in five frequency bands spanning 22 to 90 GHz, and its results form the bedrock of modern cosmology helping nail down values such as the age of the universe (13.77 billion years) and how much of the matter in the universe is "dark" (about 84%) when combined with other measurements.

Planck's more precise numbers are slightly different from WMAP's. Planck covered nine bands from 30 to 857 GHz, and it's still working in the three lowest bands. The sweet spot for observing the CMB — where the galaxy's dusty, star-studded plane is the least bothersome — is from 70 to 150 GHz, making Planck an ideal follow-up to WMAP, Planck team member Bruce Partridge (Haverford College) said last month in Boston at the annual meeting of the American Association for the Advancement of Science.

The oldest light in our universe, seen today as the cosmic microwave background, suffuses the cosmos. This all-sky map, created from all nine frequency bands of the Planck spacecraft, shows the CMB's details at a precision never before acquired. Click for high resolution (5.5 MB). See comparison with WMAP.

8. Chapter 8. What are the Alternative to Big Bang ?

[Khoury, J.;Ovrut, Burt A. ; Steinhart, P.J. & Turok, N.; "Ekpyrotic Universe: Colliding branes and the origin of Big Bang", Physical Review D, 64, 123522-123546 (2001)]. Paul Steinhardt of Princeton University and Neil Turok of Cambridge University have proposed a new hypothesis "Endless Universe-beyond the Big Bang" by Random Press.

They propose that we live in a 10-D space and 1-D time. In this 10-D space there are two 3-D Universes which are connected to each other by 7th dimension. The 7th extra dimension is the gap between two parallel objects called 3-D Branes. The visible world resides in these 3-D Branes. These two Branes are like sheets hung out to dry on parallel drying lines. Every trillion years or so, after each Universe had dissipated into darkness during expansion phase, the two would approach and collide. This would create the Big-Bang without any singularity, non-Gaussian Probability Density Graph of the primordial perturbations and without any B-mode gravitational waves radiation. Everything else will remain the same. We would still get the CMB radiation map as we are getting. There will still be continuous expansion leading to a cold Universe. But before they are dead the two universes collide and reset the clock. The cycle again begins. This goes on ad-infinitum. In this case there is no Gravity Waves radiation. Hence detection of B-Mode Polarization in CMBR will be the key to validating either of

the models. Detection of primordial Gravitational Waves will decisively hold out the BB Model.

9. Chapter 9. The Most Amazing Discovery of 20th Century- the Triumph of Monotonic M1 World Scenario Predicted by Friedmann in 1922

Two group of astronomers working independently though using the same technique of observing SNe Ia at different red-shift came to the following conclusions:

In first 8.9by after the BB, Universe was decelerating. For the

next 4.9by till now that is till 13.8by after the BB, Universe has been accelerating. That is from 0 time to 400,000y after the BB, radiation dominated the Universe. From 400,000yrs to 8.9by after the BB, matter dominated the Universe. From 8.9by onward till now (i.e. for last 4.9by) Universe has been accelerating and Universe will continue to be dominated by Dark Energy which Einstein referred to as Cosmological Constant and it arises due to Vacuum Energy which was responsible for inflationary phase of the Universe at its inception. This is evident from the data in Table 5 and from the expansion history given in Figure 18.

z	t(after BB)	Dist. From MW	remark	Universe's exp.rate
1.7	3.82by	10bly	60% brighter than predicted	decelerating
1.6	4by	9.8bly	60% brighter than predicted	
1.0	5.85by	7.97bly	60% brighter than predicted	
0.46	8.9by	4.92bly	At the correct position	Inflexion-Cosmic Jerk
0.425	9.18	4.64bly	20% dimmer than predicted	accelerating
0.4	9.38by	4.44bly	20% dimmer than predicted	

Table 5. Locations of SNe Ia at varying Red-shift and their positions with respect to the predicted positions by Hubble Law. (Reiss et.al.1998, Reiss et.al.2004)

Utilizing a simple kinematic description of the magnitude red-shift data Reiss et.al. found that SNe favour recent acceleration and past deceleration at the 99.2% confidence level. The best fit redshift of the transition between these opposite kinematic phases is $z = 0.46 \pm 0.13$, although the precise value depends on the kinematic model. From the Table 5, it is evident that

astrophysical reasons could not have been causing the dimming. Table 5 proves that in last 4 to 5by, Universe has been accelerated driven by strictly positive Cosmological Constant. SNe Ia were infact tracing the cosmic history. It was also find that Dark Energy was not evolving but keeping constant hence indeed it was Cosmological Constant.

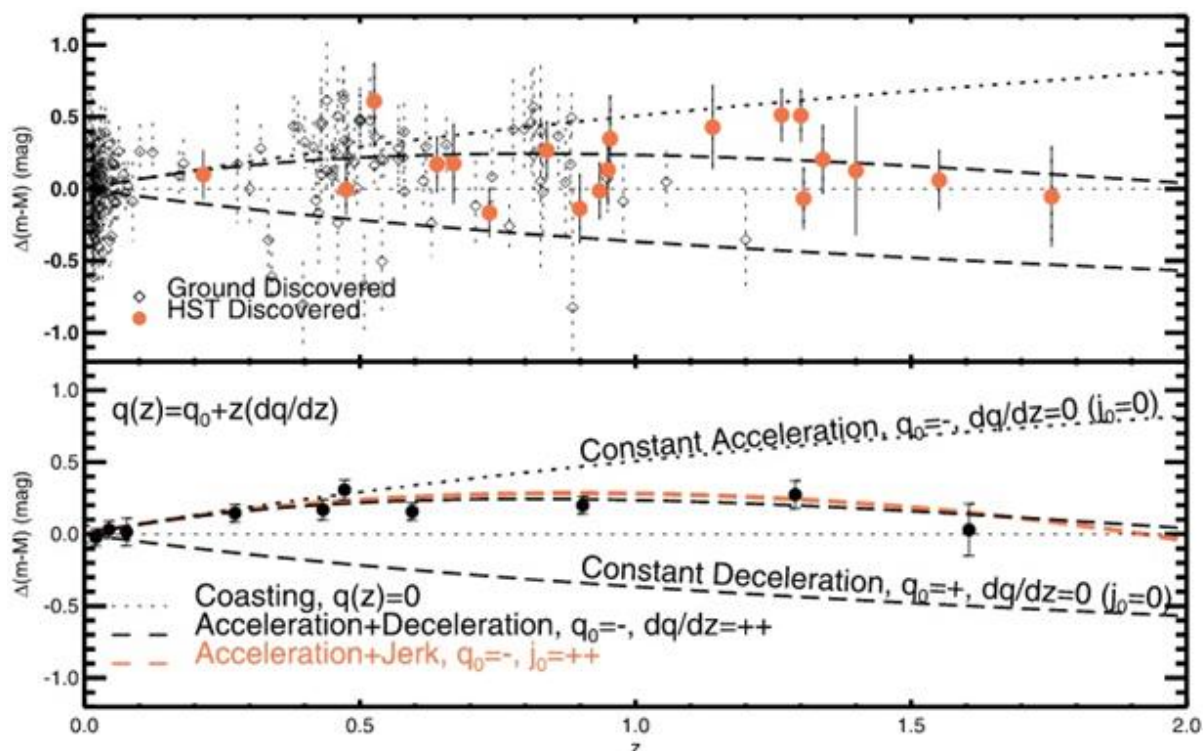


Figure 21. Top: SNe Ia from ground-based discoveries in the gold sample are shown as diamond. HST discovered SNe Ia are shown as filled symbols. Bottom: Weighted Averages in fixed red-shift bins are given for illustrative purposes only. Data and Kinematic models of the expansion history are shown relative to an eternally coasting model $q(z) = 0$. Models representing specific kinematic scenarios are illustrated. Curtsey: Reiss et.al.(2004). [Fractal86.eps]

The galaxies observed at $r = 8.4 - 10.5$ Gly away ($1 < z < 1.6$), are closer to the Milky Way than they should be, given the acceleration rate shown by the galaxies 5 Gly away. Thus,

$$R_f = \left(\frac{kc^2\rho}{2\Lambda}\right)^{1/3} R_0 = \left(\frac{0.3}{2 \times 0.7}\right)^{1/3} R_0 = 0.6R_0; \quad (22)$$

If $R_0 = 13.82$ Gly then $R_f = 8.29$ Gly.

If the Schwarzschild Radius is calculated it comes as follows:

$$R_s = \frac{2GM}{c^2} = \frac{k\rho_0 R_0^3}{2} \approx 0.6R_0; \quad (23)$$

This means inflexion point is very close to the event-horizon of the Universe. What this means is that in first 8.9Gy after the BB our Universe was Black Hole completely cut-off from the outside Universe. But after 8.9Gy, crossing the inflexion point, it became visible to other Universes.

Measuring deceleration weighs Universe. Dense Universe leads to rapid deceleration. Sparse Universe lead to gradual deceleration. If vacuum energy exceeds the inertia, Universe accelerates.

9.1 Gravity at the Largest Scale is Repulsive. *The acceleration of the Universe is probably the most profound observational mystery in our current Physics*

By using the imprint of the early sound waves in our galaxy data we can measure 'd' using a simple geometrical test. Same 'd' can be measured by SN and the correspondence can be checked. This will confirm the reality of accelerating expansion. (Komatsu et.al. 2011)

The problem of these rulers is that it can be tested on a very large scale only. We must probe Gpc-side cube. SDSS has probed only 1Gpc-side cube. BOSS (Busca et.al.2013) has done it for 2.2Gpc-side cube. It beautifully confirms the results obtained in Figure 21. The results of BOSS are plotted in Figure 17.

In the first million years of the Universe, cosmic perturbations drive sound waves into the Cosmic Plasma. These sound waves are seen in CMB maps as BAO. We have now detected the imprint of the acoustic phenomena in the clustering of nearby galaxies thereby completing an important test of our theory of gravitational structure formation. Moreover because the sound waves patterns has been seen both at low Red Shift in the Galaxies and high-z in the CMB, we can measure distance with fair degree of accuracy to these two very disparate redshifts. This yields a geometric demonstration of the acceleration of the expansion rate of the Universe (Eisenstein et.al. 2004).

Our detection confirms two aspects of BAO theory:

First that oscillations occurred at $z \geq 1090$;

Second that BAO survived the intervening times to be detected at low z.

The small amplitude of the features requires that there exists matter at $z \sim 1090$ that does not interact with photon-baryon plasmic fluid. This must be DM.

Clear evidence (3.4σ) for the acoustic peak at 100h-1Mpc scale

at some time, the Universe switched from deceleration to acceleration. The inflexion point was estimated as being at about $R_f = 5 \pm 1$ Gly ($z = 0.46 \pm 0.13$), and the M1 model triumphed.

is found. The scale and amplitude of the peak is in excellent agreement with the prediction from Λ CDM interpretation of CMB data such as from WMAP. Moreover the broadband shape of the rest of the correlation function gives a measurement of the matter density Ω_{Mh2} that matches the CMB findings.

In CDM models, primordial fluctuations grow into large scale fluctuations since $z \sim 1090$ gravitational instabilities. During the growth from $z \sim 1090$ to the present day, acoustic signatures persist. This means that primordial perturbations grow in a manner that leaves the Fourier Modes of the density field uncoupled. This protects the narrow features such as BAO as they grow. Non-linear gravitational perturbation theories generically predict mode coupling that would wash out the BAO signature (Fry 1984, Goroff et.al. 1986, Jain & Bertschinger 1994).

Detection of low-redshift BAO is a stark confirmation of the CDM theory for the growth of Cosmological structures and it also establishes the link between CMB anisotropies and the matter perturbation.

The narrowness of the acoustic peak in real space offers an opportunity to measure distances to higher red-shifts. BAO improves the signal to noise ratio data in the clustering statistics. This improvement makes a super linear improvement in the distance constraint. This measurement provides a geometric evidence of Dark Energy as well as DM. Previously we had only gravitational evidence. The size of the acoustic peak is predicted by the co-moving distance that a sound wave can travel between the hot spots (generator of the perturbation) and also by the epoch of recombination at $z \sim 1090$.

Once established at $z > 1090$, the acoustic scale can be used at low z as a standard ruler on equal footing to any other distance ruler.

10. Chapter 10. BAO and the Standard Theory of Cosmology

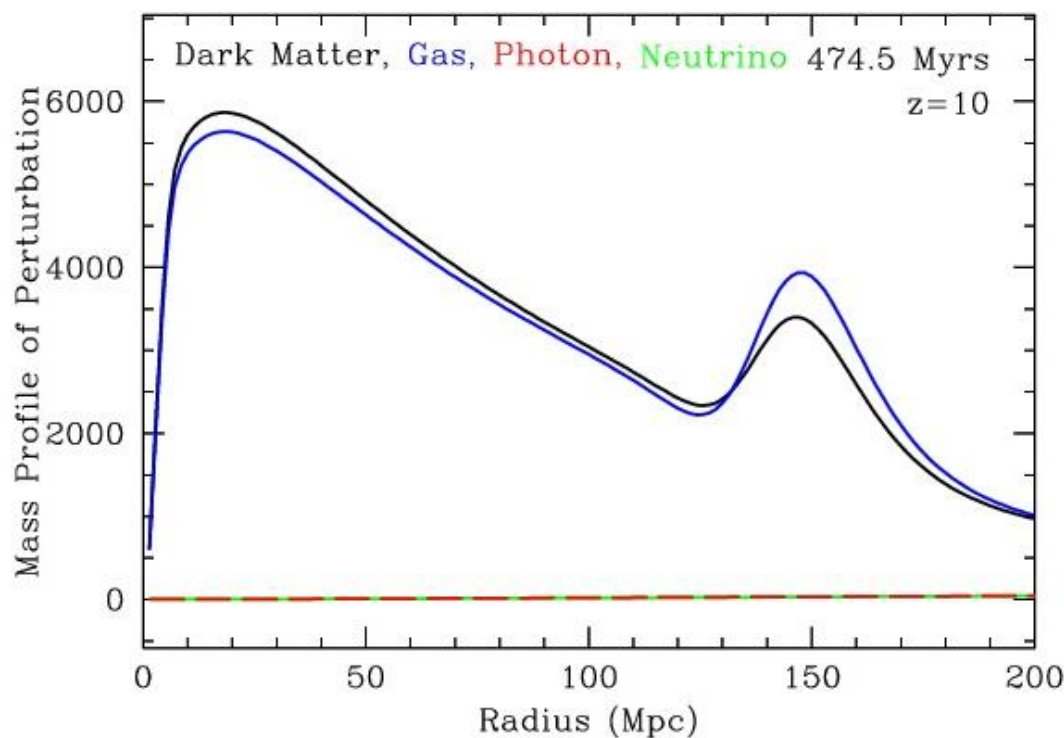
In over-dense region, self-gravity wins in relation to expansion hence it leads to a cumulative build up. In under-dense region, matter is removed to over-dense region leading to a complete void in the under-dense region. In 1 million years, density perturbation lead to BAO. This gives rise to the characteristic angular scale of 1° and famous acoustic peaks also called Doppler or Sakharov Peaks.

Attempts were made to measure the acoustic peaks. The peaks

correspond to large scale variation in the early Universe that are created by gravitational instabilities resulting in acoustical oscillation in the plasma. The first acoustic peak was detected by TOCO experiment and the result was confirmed by BOOMERanG and MAXIMA experiments. These measurements demonstrated that local Universe is flat and Cosmic Inflationary Theory was the right theory of structure formation. WAMP detected the second and third peak.

The same BAO creates a small residual imprint in the present day clustering. In CMB we find patterns of over-density (hot spot)

and under-density (cold spots). Universe contains DM, Baryonic Matter, Photons and neutrino. Since initial perturbations are assumed to be adiabatic, hence all the species are perturbed by the same amount. So small density fluctuation in Baryonic Matter will cause the same perturbation in DM, photons and neutrinos. In fact photons and neutrinos are ultra relativistic hence they have energy perturbation about 4/3 bigger than those of DM and gas. In course of time the two look the same. The spherical shell of gas has imprinted itself on DM. Since DM outweighs gas by 5 times hence the acoustic peak decreases in contrast as gas comes in lock-step with DM as seen in Figure 15.



In course of time the perturbation in the Dark Matter and the Baryonic Matter look similar. The spherical shell of the Baryonic Matter has imprinted itself in the Dark Matter distribution. This is known as the acoustic peak. The acoustic peak decreases in contrast as the gas comes in lock-step with the Dark Matter simply because it outweighs the gas by 5 to 1.

Figure 15. Fractal 59. At 474.5My after the BB, acoustic peak decreases in contrast as the gas comes in lock-step with Dark Matter simply because latter outweighs the gas by 5 to 1.

11. Chapter 11. Birth and Evolution of Stars (Dunlop 2011, Tolstoy 2011)

All stars have one thing in common and that is nuclear fusion. When a solar nebula is born then it can give rise to asteroids, planets, brown dwarfs or stars or a combination of these objects. An accretion of gas and dust is a planet if the mass is below 13mJ (mJ = mass of Jupiter) A typical planet is either a Gas-Giant, an ice-Giant or a rocky planet like Earth.

An accretion of gas and dust between 13mJ and 75 to 80mJ is a Brown Dwarf. It is called a sub-stellar body but technically it is a failed star where hydrogen fusion cannot be sustained.

Above 80mJ, a full fledged star is born where the gravitational collapse leads to Helmholtz Compression and heating, leading to Nuclear Fusion of Hydrogen. The energy released during the

nuclear fusion checkmates the further collapse and the fusing star mass reaches a temporary equilibrium.

When the core reaches 15MegaKelvin temperature Hydrogen fusion starts. Through Carbon-Nitrogen-Oxygen cycle Hydrogen is converted into Helium. [Hagger,Alexander ;“Going Supernova”, Nature 494, 46-47, (7th February 2013)]

When Hydrogen, the reactor fuel, is exhausted then energy release is stopped and gravitational collapse sets in until a core temperature of 100MKelvin is reached. At this point Helium fusion into Carbon by Triple-Alpha Process is ignited.

When Helium, the reactor fuel, is exhausted then energy release is stopped and gravitational collapse sets in again until a core temperature of 600MKelvin is reached. At this point Carbon

fusion into Neon by Carbon Burning Process is ignited. When Carbon, the reactor fuel, is exhausted then energy release is stopped and gravitational collapse sets in again until a core temperature of 1200MKelvin is reached. At this point Neon fusion into Oxygen by Neon Burning Process is ignited. This transformation is completed in hundreds of years and this stage is reached in stars heavier than 6 to 7M_o. When Neon, the reactor fuel, is exhausted then energy release is stopped and gravitational collapse sets in again until a core temperature of 1500MKelvin is reached. At this point Oxygen fusion into Silicon by Oxygen Burning Process is ignited. This stage is reached in stars heavier than 8 to 10M_o.

When Oxygen, the reactor fuel, is exhausted then energy release is stopped and gravitational collapse sets in again until a core temperature of 2700 to 3500MKelvin is reached. At this point Silicon fusion into Nickel-Iron by Silicon Burning Process is ignited. This nucleosynthesis is completed in weeks.

Once Silicon is exhausted a gravitational collapse again sets in which is unchecked because Iron is most tightly bound nuclei

and its fusion reaction is endothermic. It does not release energy hence no newer type of Fusion Reaction can set in. The star core is in a free fall condition or in a runaway Gravitational Collapse. The star at this point achieves an onion like multi-layer structure with Hydrogen-Helium in the outer most layer and Nickel-Iron at the core.

Heavier stars have a short span because they quickly burn away their fuel whereas lighter stars have long life span like our Sun which has life span of 10Gy. It has survived for 5Gy and it will survive for another 5Gy. Universe age also known as Hubble Age is 13.8Gy. Our Milky Way is a spiral galaxy which is 10Gy old. In the Milky Way Sun is probably third generation star. The solar nebula was born 4.567Gy ago. From this Solar Nebula, Sun, Planets, Asteroids, Comets in Oort Cloud and Kuiper Belt Objects (KBO) were born.

In Table B.1 we give the final three alternative destinys which the stars can achieve.["We are cosmic dust but you are everything to me", Kelly Oakes, July 21, 2011]

Mass of the star	Type of Explosion	Mass after the explosion	The process which checkmates the collapse	Type of remnant.
Sun-like	Nova	Less than 1.4M _o	Electron degeneracy	White Dwarf
Less than 20 M _o	Supernova	1.4M _o to 3M _o	Neutron degeneracy	Neutrinos take away the heat hence a stable Neutron Star is formed with 20km dia.
20 M _o >M>50 M _o	Supernova	Greater than 3M _o	Quark degeneracy /?	Black hole
M>50 M _o	Directly collapses into BH	Greater than 3M _o	Not Known	Black hole
M>140 M _o	Pair-instability SN	Not Known	Not Known	No Black Hole

Table B.1. The three alternative fates of a star in its death.

Type of remnant	Matter density	Mass	Diameter
White Dwarf	10^9 Kg/m^3	Less than $1.4M_{\odot}$	12000km
Neutron Star	10^{17} Kg/m^3 (density of the nucleus)	$1.4M_{\odot}$ to $3M_{\odot}$	20km
Black Hole	Not Known	Greater than $3M_{\odot}$	Event horizon

Table B.2. The properties of White Dwarf, Neutron Star and Black Hole

12. Chapter 12. Evolution of Stars and Galaxies

The earliest stars and galaxies were made of pristine materials and they are called Population III stars. They primarily had Hydrogen and Helium with traces of Lithium and Deutrium. After the death of Population III stars, heavier elements were introduced through Novae explosions and Super-Novae explosions. Carbon, Neon, Nitrogen, Oxygen, Silicon, Nickel and Iron are introduced in the Universe through Novae explosions. These elements have been nucleosynthesized in the cores of all stars during their Main-Sequence existence. Calcium, Magnesium and Titanium and other radioactive elements were synthesized in Super-novae explosions and strewn around the Universe subsequently. In 1950, M. Burbidge, G. Burbidge, W. Fowler, F. Hoyle expounded the theory of Nucleosynthesis.

It became clear by theory as well as by careful observations also that as we move from Population III to Population II and now in Population I stars we find that over time with each successive generation of stars and their novae or supernovae deaths the gas in galaxies, from which the stars are formed, become enriched in heavy elements. Hence we conclude that metallicity [% of heavier elements as well as alpha elements abundance = $\alpha/\text{Fe} = (\text{Ca} + \text{Mg} + \text{Ti})/\text{Fe}$] have steadily improved. Through the study of nearby galaxies it has been concluded that Milky-way and its like can retain the enriching products of Super-novae explosions and rapidly build up metals and alpha elements in its disk, bulge and halo. This is not the case with nearby Dwarf Galaxies.

Our neighboring dwarf Galaxies have difficulty retaining gas and products of star formation. This results in large scatter in abundance ratios as well as much slower build-up in alpha elements in Dwarf Galaxies. We also conclude that the bulk of stellar mass of Population I and II galaxies cannot have come from the merger of two galaxies but that most have come from

the gas within the bulge of the galaxy. This means that in first 1 Gy (that is at z , redshift, = 5 or larger- see Appendix D) after the Big-Bang according to the current theory of hierarchical structure formation smaller structures (dwarf galaxies) may have merged to form the larger galaxies but in Population I and II smaller galaxies merger is an exception.

12.1 The Results of the Studies Conducted by Sloan Digital Sky Survey (SDSS)

Sloan Digital Sky Survey Programme has calibrated the optical spectra of 1 million galaxies in the Local Universe. Most massive galaxies are the oldest, generally elliptical, have very little recent star formation histories and the spectra of the galaxy can be explained in terms of one to three distinct stellar populations namely bulge, disk and halo population.

Typical masses of galaxies have younger average stellar ages, more complicated star formation histories and the overall spectra can be explained in terms of five distinct stellar populations namely extreme disc, thin disc, thick disc, bulge and halo.

This means star formation rate was very high initially and then it monotonically declined. Star formation has in effect moved from most massive galaxies to less massive galaxies.

Here the question arises as to why star formation has stopped in most massive galaxies?

In last twenty years we have built a large number of ground-based giant telescopes of 8 to 10 m diameter. We also have space telescopes such as Hubble Space Telescope, Spitzer Space Telescope and Herschel Space Observatory. Study of young massive stars provide the most useful tracers of star formation activity as enumerated in Table B.3.

Tracer number	1	2	3	4
Property of the tracer	Bright optical-UV continuous light from star themselves	Bright H ₂ & O ₂ emission lines from the surrounding gas ionized by the hot stars	Enhanced emission at Mid & Far infra Red from the dust warmed by UV light from the stars.	Radio-emission from the relativistic electrons accelerated by the shock waves produced by Supernova explosions.

Table B.3. The useful tracers of star formation activity in Young Massive Stars

12.2 Star Formation Rate through the Cosmic Times (Peebles et.al. 1994, Hogan 1996)

After extensive studies particularly those of Sloan Digital Sky

Survey(SDSS) we have arrived at the Figure B.1 (given in Chapter 1) and concluded the following results in Table B.4:

Time after BB	Z [†] (redshift) Or T(Kelvin)	Event	Comment
0 year	Infinite	Big Bang occurs	Time is born with Big Bang
10 ⁻⁴³ s	3.16×10 ³¹ K	1 st Symmetry breaking	Quantum Gravitation to GUT phase transition. Relic gravitons left out.
			Density of matter = 10 ⁹³ gms/cc.
10 ⁻³² s		Inflationary Phase ends	Primordial perturbations in matter-equivalent energy density freezes out.
10 ⁻¹⁰ s	10 ¹⁵ K, 100GeV	2 nd Symmetry breaking	GUT to Electro-Weak Phase transition, weak force decouples, relic intermediate vector bosons left out, Universe filled with a soup of quarks, leptons, photons. Baryonic Number freeze out takes place and separation of radiation density and matter(DM+BM) density is formalized.
10 ⁻⁶ s	10 ¹³ K, Less than 1GeV	Fission of nuclear particle stops	Quark-nucleon phase transition. Universe filled with a soup of leptons, nucleons, photons. Relic quarks left out. Density of matter = 10 ¹⁸ gms/cc.

10^{-4} s	10^{12} K 1000×the core temp of Sun	Instability of leptons lead to instability of nucleons.	Continuous transmutation taking place between proton and neutron. Density of matter = 10^{14} gms/cc.(nuclear density)
4sec	5×10^9 K	Leptons become stable hence nucleons stabilize.	p, n stabilizes to 7:1
3min	745×10^6 K		75%H ions,25% He ions
15mins	333.3×10^6 K	Nuclear fusion first stage completed.	Matter in plasma form stabilized at 75%H ions,25% He ions or 92% and 8% by atomic number density with traces of Lithium
<p>From here onward Universe enters the Dark Ages. But the matter is not uniformly distributed as confirmed by the study of Cosmic Microwave Background Radiation through COBE , WAMP and Planck Mission. The denser part of matter shows up as red in CMBR map and rarefied part shows up as blue. The denser part are the seeds of stars, galaxies and clusters which have followed bottom-up model of hierarchical formation based on ΛCDM Model. CMBR carries the imprint of the matter distribution at the time of decoupling which will occur at 370,000 years after the BB because temperature cools below 4000K which allows plasma to neutralize. Dichotomy of DM and BM leads to Baryonic Acoustic Oscillation generation from the hot spots.</p>			
7,000yrs	$Z = 10,000$	Dark Matter decouples from plasma	From this point onward DM starts evolving into halos and sub-halos
370,000yrs	$Z = 1090$, 4000K	Plasma recombines into cold, neutral, dark universe.	Temperature of the Universe falls to 4000K where all ions recombine to form neutral atoms and molecules of H_2 and He. Gravity will dominate from now on.
The stage is set for the formation of Population III stars and galaxies.			
200My	$Z = 18$	First stars and galaxies born	Universe reionizes.
500My	$Z=8.5$	Not Known	Not Known
600My	$Z=7$	Dark age ends and the epoch of re-ionization begins	Population III stars and galaxies are formed and these re-ionize the cold, neutral and dark universe.(detected by near-IR Wide Field Camera3 mounted on Hubble Space Telescope).

Population III stars were massive and hence short lived however through internal fusion followed by supernova explosion they must have commenced the process of chemical enrichment through recycling in the interstellar matter. This produced the successive generations of Population II and Population I stars with progressively higher metallicity and alpha elements.			
1Gy	Z=6	Rapid build-up of low metallicity stars.	Here heavier elements reside in cool gas and dust grains within the Galaxies.
2Gy	Z=3	Metallicity increases through nuclear synthesis. Star formation Rate = $\rho = 0.2^*$	Heavier elements reside in stars , planets and interstellar gas. There is possibly a peak in Star Formation Rate.
3Gy 4Gy	Z=2 Z=1	Half the stars were in place and $\rho \geq 10 \rho_0$ Rate of star formation is $10 \rho_0 = 0.1^*$	Population II & Population I stars and Galaxies are born. Milky Way is born at this time. It is the third Generation Galaxy(Population I).
8.8Gy	Z = 0.46	Cosmic Jerk	Till this point Universe expansion rate was decelerating. From this point onward expansion rate is accelerating due Vacuum Energy Density being greater than (Radiation Density + Matter Density).
9.133Gy	Z = 0.43	Our Solar Nebula is born.	Our Sun is Population I star.
13.7Gy (present)	Z=0	Rate of star formation is $\rho_0 = 0.01^*$	

Table B.4. The Cosmic History of Star formation

*Units of star formation rate is (MSUN) $\times y^{-1} \times \text{Mpc}^{-3}$, ρ_0 = present day star formation rate;

†Distance calculation from Redshift (z) is given in the Question 8 of the Background material..

13. Chapter 13. Formation and Evolution of Galaxies (Milky Way Researchers 2011, Heckman & Kauffman 2011)

Through the advancement of γ -Ray and X-Ray astronomy it has been possible to peer into the nuclei of several galaxies and through the study of the last decade it is confirmed that probably all the Galaxies have Super Massive Black Holes(MBH). It is confirmed that the lives of Galaxies and MBHs are inextricably

intertwined. It can also be said that as the galaxies grow so do the MBH at the center.

Quantum Mechanical fluctuations in the Universe emerging from the Big Bang gave rise to the small inhomogeneities which acted as the future seeds of the super clusters, cluster and galaxies. These inhomogeneities attracted the surrounding

matter gravitationally and grew into clumps called haloes. In these haloes there is gravitational heating as we see in Pre-Main Sequence Stars and there is radiative expansion and cooling. The two are trying to compensate each other. If gravitational heating dominates there will be subdued star formation and if radiative cooling takes place then there will be rapid star formation.

In low-mass haloes below critical mass $10^{12}M_{\odot}$, cooling dominates and there is a star formation burst due to cold gas inflow. This is how the spiral galaxies grow by gas accretion. In high-mass haloes above $10^{12}M_{\odot}$, heating dominates and growth stops by accretion. Halo mergers take place leading to large haloes. Within the large haloes galaxy mergers take place and spiral galaxies disks are scrambled into bulgy elliptical galaxies.

Most MBHs are turned off or dormant. But if there is a disc of accretion, the gas and dust within the radius of influence will be sucked into the BH just as a vortex in a river sucks in the surrounding water. When the reservoir of gas and dust is exhausted this accretion will stop and BH will shut-off. In-falling gas and dust emits radiation in γ -ray, X-Ray, Ultra-Violet and optical part of the spectrum. These AGN are seyfert galaxies (Fritz et.al.1971).

Apart from these emissions there are conical relativistic jets being emanated from the poles of the BH (McNamara et.al. 2007). Unsteady accretion flow gives rise to variable AGN. The most variable AGN are a sub-class called Blazars with typical masses of 10^8 to $10^9 M_{\odot}$. It is radio and optically bright but luminosity is dominated by X-ray and γ -ray. Doppler beam emitting region within a jetted outflow moving relativistically causes changes on minutes- to hours- time scale. The high energy emission is caused by Inverse Compton Up-Scattering of accretion disk photons. The conical emanation takes place in Super Massive Black Hole engulfing a large amount of surrounding gas and dust (Ulrich et.al.1997, Maraschi et.al.2003, Bottcher et.al.2007, Fossati et.al.1998). The same kind of jets can be emanated from Massive Black Hole which is tidally shredding the star launched on a death spiral towards the nucleus of the Galaxy (Bloom et.al.2011, Levan et.al. 2011). The two conical jets are very narrow streams of particles travelling in opposite directions at relativistic speeds. These relativistic jets travel out to large distances across the Galaxy.

As they emerge out of the two poles of the galaxy they finally decelerate as they interact with the interstellar gas and dust and they turn on two radio-emitting lobes. This kind of Active Galactic Nucleus(AGN) is called QUASERS as shown in the Figure C.3.



Figure C.3 Twin jets produced by the supermassive black hole in the galaxy Messier 84 are strongly interacting with the hot tenuous gas in the galaxy's halo. The black hole is located at the center of the brightest region in this image. The jets are traced by their radio emission (shown in red) as mapped with the Very Large Array (VLA), and the hot gas is traced by its x-ray emission (shown in blue), as mapped with the Chandra X-ray Observatory. The jets decelerate as they travel out into the halo and light up as two lobes of radio emission. These lobes form two cavities in the hot gas as they push it out of their way. [Source: x-ray, NASA/Chandra X-ray Center (CXC)/Max Planck Institute for Extraterrestrial Physics/A. Finoguenov; radio, NSF/National Radio Astronomy Observatory/VLA/European Southern Observatory/R. A. Laing; optical, Sloan Digital Sky Survey]

The Star population converts 0.7% of Solar Nebular Matter into energy by nuclear reaction from which it has been born. In contrast SMBH in AGN accretes 10% of the rest mass in the bulge of the Galaxy and converts it into energy. Hence they (AGN) stand out as distinct cosmic beacons clear across the Universe. Through such beacons, distance estimate can be made for the far flung Galaxies. Detection of GRB090429B, the most distant GRB(Gamma Ray Burst), is a case in point (Cuchiara et.al. 2011) and these beacons will also let me know how the SMBH have evolved across the entire span of cosmic time. We have different categories of AGN and accordingly we

have different categories of Galaxies such as Seyfert Galaxies, Blazars and QUASERS. All these three play an important role in anchoring Clusters and Super-Clusters.

Even a tiny fraction of (<1%) of this energy released within each bulge could heat and blow away the entire gas content from the bulge and completely stop star formation.

13.1 Classification of Galaxies by Galaxy Zoo

Galaxy Zoo was an online classification program for all the galaxies catalogued by Sloan Digital Sky Survey(SDSS) over a period of 11 years. The results have been tabulated in Table(C.1).

	Blue (indicative of star formation)	Red (star formation quenched)	
Spiral Galaxy	80% Here gas component is large hence star formation is high.	20%_these are barred red spirals. Hydrogen is being siphoned off from the halo and star formation is retarded	
Elliptical Galaxy	20%_these are recently formed small galaxies and are undergoing vigorous star formation.	80% These lack gas hence star formation has stopped. Only old light mass stars are there.	
Little Green Galaxies			Compact galaxies. These undergo extreme star formation and emit light at a wavelength that is characteristic of highly ionized oxygen . In SDSS images these appear green.

Table C.1. Classification of Galaxies based on the Galaxy Zoo program

Astronomers have concluded that galaxies are formed when dark matter clusters together under its own gravity and then pulls gas, dust, stars and smaller galaxies to form the flat extended disk of a spiral galaxy. Dark matter stays in the spherical “halo” that surrounds the whole galaxy. In spiral galaxies, stars keep forming in the disk as neutral gas rains down from halo into the spiral arms.

Elliptical galaxies result when two galaxies of comparable masses collide- if one or both are spiral galaxies, the spiral structure is destroyed and stars are left in random orbit around the galactic center. The collision also slam together gas clouds causing burst of intense star formation that flares and burns out quickly using up all the hydrogen gas. The end result is a structure less blob of a galaxy with no gas clouds and few young stars.

Galaxies grow by accretion of surrounding cool gas in the halo or the merger between two or more galaxies. This merger takes

place in seven distinct steps:

- Two galaxies merge together as shown in Figure E.11, Appendix E. Thin and highly ordered disk components are scrambled together.
- Tidal forces between the two galaxies drain away angular momentum from the cold gas in the disk of the galaxy, allows the cold gas to flow into the inner region and then fuels an intense burst of star formation. This flow delivers a fresh supply of gas to SMBH as shown in Figure E.12.
- The scrambled disk material settles into a newly created bulge.
- If the two progenitors had their own BH then the two also merge to give rise to a new BH as shown in Figure E.13.
- The release of energy from the merger induces a star formation burst so intense that it may blow away most or all remaining gas in a powerful outflow.
- Relativistic conical jets from SMBH will pump energy into the surrounding gas preventing it from cooling and falling into the galaxy thus quenching star formation.

vii. Finally we have a single Galaxy with a larger bulge and a larger SMBH as shown in Figure E.13.

viii. Living Galaxy has reached its limit of growth and it becomes passive. Star formation stops. BH growth also stops.

Growth rate of Galaxies and SMBH depend strongly on mass (Panter et.al.2007). As we see in Figure E.17, in Appendix E, most massive galaxies and their respective SMBHs grew rapidly early in the cosmic history and then they stopped growing after reaching a limit. In contrast as seen in Figure E.18, lower mass galaxies and their respective BHs have grown at a lower uniform rate throughout the entire cosmic history.

Apart from these major mergers there are minor mergers. Our Milky Way has assembled itself from a kit of hundred of Galactic building blocks. Whenever a small galaxy or a star cluster passes by too close, our Galaxy's gravity tears it apart and draws it into the main galaxy (Ibata et.al. 2007, Purcell et.al. 2011). Our Milky Way's, and so Galaxy's in general, tangled history of merging and accreting have brought new stars, gas and dark matter within the halo of our Milky Way. In fact merger and accretion are processes which have become the main driver of Galaxy formation and evolution. These minor mergers have also revealed the nature of dark matter- its hydro-static equilibrium shape and its granularity.

13.2 Different Classes of Galaxies According to the Mass of BH (Heckman et.al. 2011)

Mass of BH	Accretion disc	Spin Rotation	spectrum	Name of the galaxy
$10M_{\odot}$		Not Known	Not Known	This is not the fulcrum of the galaxy and is the result of the death of a massive star of mass $> 20M_{\odot}$.
10^5 to 10^6M_{\odot} (moderate BH)	No	Little or no	quiet	Fulcrum of light weight Galaxy
10^5 to 10^6M_{\odot} (moderate BH)	Yes	Yes	IR to γ -Ray continuous	Fulcrum of Seyfert galaxy.
10^6 to 10^8M_{\odot} (SMBH)	Yes. Rate of BH growth/ $\rho_{SFR}^* = 1:1000$	Yes	More luminous and radio loud.	Fulcrum of Intermediate galaxies.
10^8 to $10^{10}M_{\odot}$ (UMBH)	No. Lack cold, dense gas.	Not Known	Switched off	Fulcrum of massive galaxies. Buried in aged Galaxies with little or no reservoir of cold, dense gas.
10^8 to $10^{10}M_{\odot}$ (UMBH)	Mass ratio of SMBH/Mass of the bulge = 1:1000 Surrounded by a halo of hot and tenuous gas		Switched on.	Fulcrum of massive galaxies. Active Galactic Nuclei (AGN)†. It has relativistic jet and strong emissions. It heats the surrounding gas. This shuts off the star formation

Table C.2. Classification of Galaxies according to the mass of the BH.

* ρ_{SFR} = star formation rate. †AGN can be a sub-class of Blazer or it can be QUASER

There is a strong connection between Star Formation Rate (ρ_{SFR}) in the bulge and the growth rate of SMBH. When there is a sufficiently large reservoir of cold, dense gas then both processes are supported.

The self-regulating process which keeps Mass ratio of (SMBH/Mass of the bulge) = 1:1000 or which keeps Rate of BH growth/ $\rho_{SFR} = 1:1000$ is by feedback mechanism as given below:

i. In Galaxies hosting 10^8 to $10^{10}M_{\odot}$ (UMBH), powerful relativistic conical jets are created which prevent the in-fall of cool gas into the bulge. Hence star formation is quenched and growth of SMBH is stopped.

ii. In intermediate mass Galaxies hosting 10^6 to 10^8M_{\odot} (SMBH), SN explosions due to the death of newly formed massive stars causes an out-flowing galactic wind. This sweeps away Galactic gas into the halo where it is in hot form. This also regulates the availability of cool gas in the bulge thereby regulating the star formation rate and growth rate of MBH to the ratio 1000:1.

iii. In a living galaxy or young galaxy, stars formation is going on and accretion of gas and dust on the BH is also going on. The accretion by BH leads to Gamma Ray Burst (GRB) and relativistic Jets. Gamma Ray Bursts are the Universe's most luminous explosions emitting more energy in a few seconds than our Sun will during its energy producing life-time.

Massive stars collapse into Black Holes surrounded by a dense hot disk of gas. The in-falling matter is diverted into a pair of high energy conical jet particles from the poles of BH that tear through the collapsing star. The jets move upward at 99.9% of the speed of light. The jet of particles strikes the gas beyond the star to produce after glows. “Catching these afterglows before they fade is the key to determine the distances of the bursts. “GRB090429B has qualified as the most distant galaxy till date (Cucchira et.al. 2011). It was detected by its Gamma Ray Burst. It is at 13.14 billion light years distance with date of occurrence at 520My after the Big Bang when the Universe was 4% of the present age and 10% of the present size. This is the first galaxy to form after the Big Bang.

James Well Space Telescope due to launch in 2017 has been carefully engineered for studies in the early Universe. An after glow spectrum from this facility would be an unique and valuable source of data.

Penn State University, South West Research Institute, Cornell University have proposed JANUS explorer to be launched by 2017. This will be used for understanding the first galaxies and the various processes guiding their formation.

By discovering and observing the most distant GRBs and QUASERS and measuring their distances autonomously without the need for follow up observation, JANUS would provide a steady stream of rewarding targets to James Well Space Telescope and ground based telescopes.

Nothing else illuminates the conditions in the early Universe like its brightest lights the GRB and QUASERS.

Massive stars are dying , leading to SN explosions. The strong emissions from SN explosions and relativistic jets are heating up the gas in the halo and SN explosions are powering an outward galactic wind that can sweep out the Galaxy’s gas and sweep it into the halo. For a given black hole mass, there is a maximum AGN luminosity, called the Eddington limit, above which the radiation-pressure force outwards exceeds the gravitational force inwards, suppressing the gas flow onto the black hole. The velocity dispersion is the bulge property that is most closely linked to the black hole because it determines the depth of the potential well from which the gas has to be expelled, and thus the minimum black hole mass for feedback. At the Eddington Limit , star formation is halted as well as the growth of black hole is stopped and Galaxy is switched off. Young and living Galaxy is turned into aged and passive galaxy. This self-regulating process has kept the mass ratio pinned down to 1:1000 in the early galaxies and keeps Rate of BH growth/ ρ SFR= 1:1000 in the present day galaxies.

There is always fresh cool and dense gas coming in the bulge from the outer disk subsequently. There is also the remnants of the dying stars being fed into the bulge. Both these factors eventually may rejuvenate the dormant galaxy.

90%	No conical jet of energetic particles		
10%	Have conical jet	Radio Galaxies, Quasars and Blazers	

Table C.3 Classification of AGN

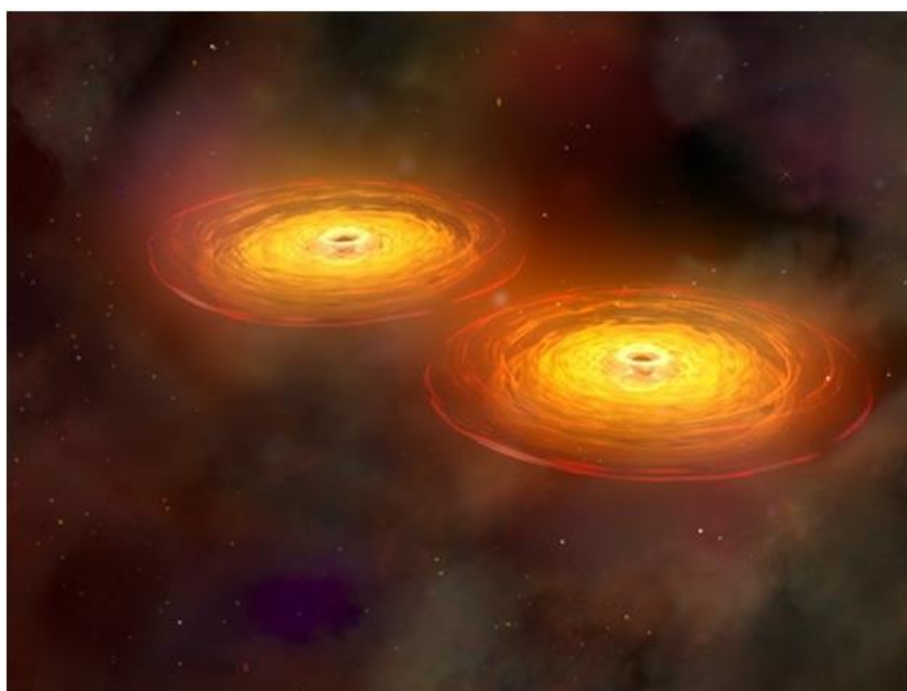


Figure E.11 Second stage in the merger of the primary and secondary Galaxies. The two galaxies are spiraling around the barycenter and moving closer together. (Illustration: NASA/CXC/M.Weiss)

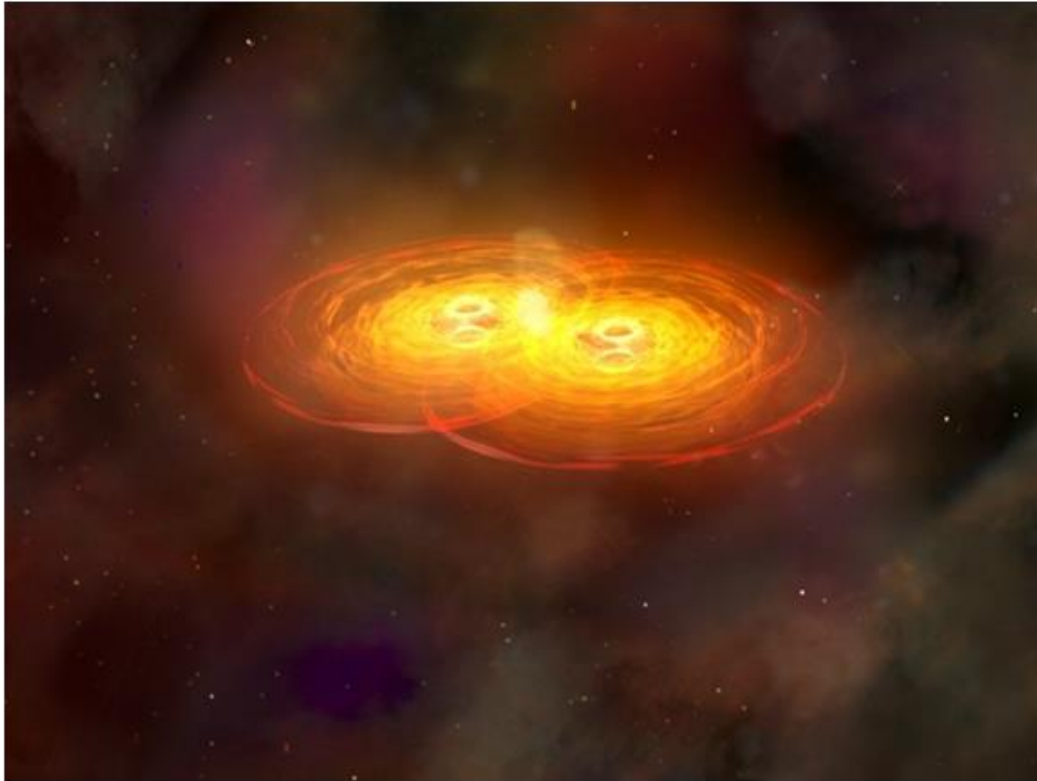


Figure E.12. In the advanced stage of merger when the two Galaxies are overlapping and interpenetrating. The two SMBHs are distinguishable surrounded a single merged Galaxy. (Illustration: NASA/CXC/M.Weiss)

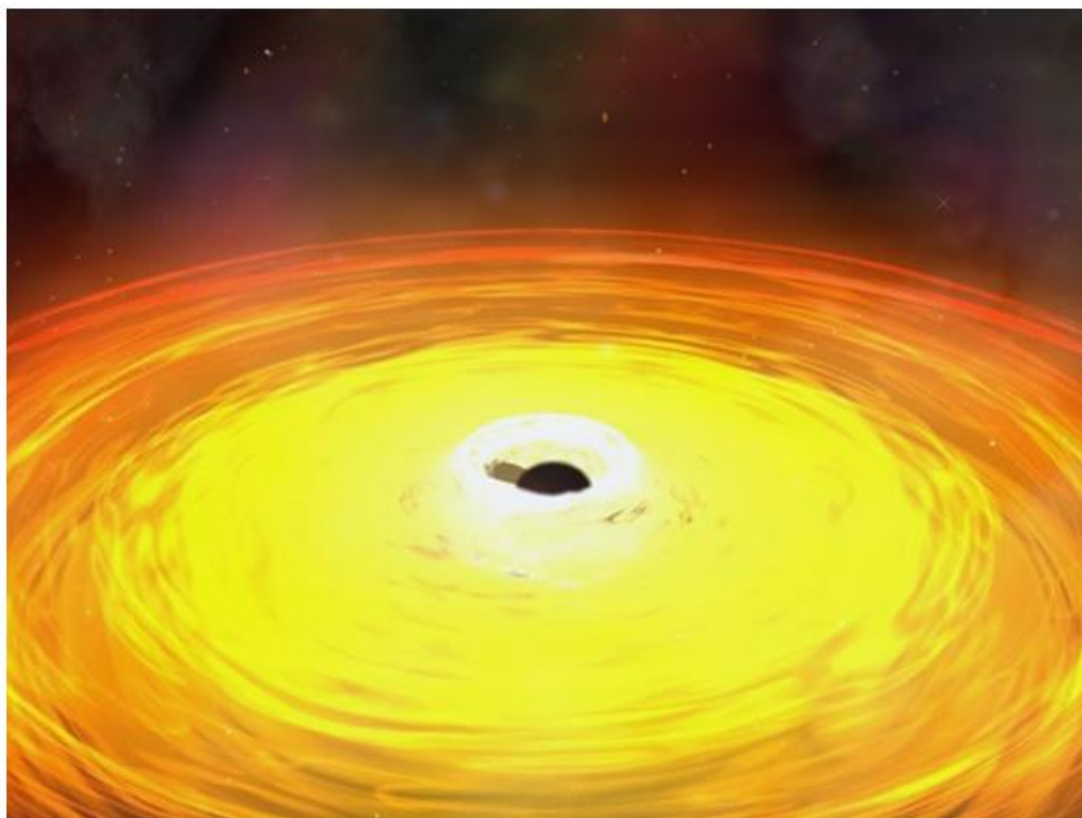


Figure E.13. The two SMBHs spiral around the common barycenter until they coalesce into a single SMBH. (Illustration: NASA/CXC/M.Weiss)

Different orientation of observation also gives rise to different galaxies.
 If we look down the conical barrel of emission then we have Quasars and Blazers,
 If we look broadside then we have Seyferts Galaxies

	Nucleus brightness variation time scale	Spectrum	At the nucleus	Total luminosity
Seyferts Appendix E. Figure E.14	months	Continuous, absorption lines, strong emission lines of H and also of O	Shoot out narrow beams of energetic electrons producing synchrotron radiation.	$10^{10}L_0$
QUASER Figure C.1	X-ray variation in days, hours ,mins	Continuous, absorption lines, strong emission lines of H and also of O	It outshines the stars. It has relativistic conical jets and two radio lobes	$10^{12}L_0$
Blazers Appendix E. Figure E.15	Optical variation over days.	High radio brightness, high optical polarization Widest range of frequencies from radio to γ -Ray.	It has relativistic jets pointed to Earth	

Table C.4. Classification of Seyferts, QUASERS and Blazers

- Two sub-groups of Blazers:
 - i. Sources showing strong and broad emission lines, such as those of quasars (called Flat Spectrum Radio Quasars).
 - ii. Sources showing a featureless optical spectrum (called BL Lac objects) (Urry 1998).

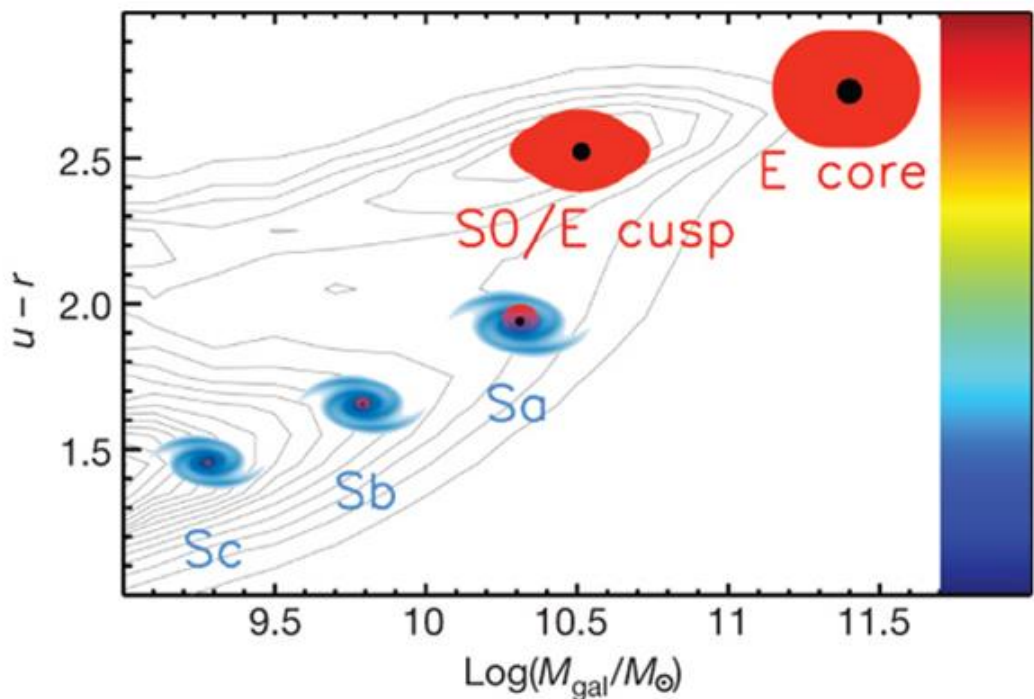


Figure C.1. The contours show the galaxy distribution on a stellar mass (M_{gal}) – colour diagram. The difference between ultraviolet luminosity and red luminosity, quantified by the magnitude difference $u - r$, is a colour indicator; larger values of $u - r$ correspond to redder galaxies. The colour bar has been inserted to convey this notion visually and has no quantitative meaning. Galaxies are classified into two main types: spirals that mainly grew through gas accretion ('S', shown in blue) and ellipticals that mainly grew through mergers with other galaxies ('E', shown in red). 'S0' galaxies are an intermediate type, but we assimilate them to ellipticals. Spirals have central bulges, shown in red, that resemble miniature ellipticals. All ellipticals and bulges within spirals contain a

central black hole, shown with a black dot. Moreover, ellipticals and bulges within spirals have the same black-hole mass to stellar mass ratio, of the order of 0.1%. This is why we call them 'bulges' indiscriminately. In contrast, there is no connection between masses of black holes and masses of disks (the galactic component shown in blue). Spirals and ellipticals are separated by a colour watershed at $u - r \approx 2$ and a mass watershed at $M_{gal} \approx M^* \approx 10^{10.5} M_{\odot}$. M^* is of the order of $fb_{crit} t$, where $M_{crit} \approx 10^{12} M_{\odot}$ is the critical halo mass for gas accretion and $fb \approx 0.17$ is the cosmic baryon fraction. Spirals form a sequence where the bulge-to-disk ratio tends to grow with M_{gal} (Sc, Sb, Sa). Ellipticals have two subtypes: giant ellipticals with smooth low-density central cores formed in mergers of galaxies that have long finished their gas ('E core') and lower-mass ellipticals with steep central light cusps formed in mergers of galaxies that still have gas ('E cusp'). Whereas core ellipticals formed all their stars over a short time span at high redshift, the formation of the lower-mass cuspy ellipticals from the 'quenching' and reddening of blue galaxies continues to low redshift. [This Figure is from the article: "The role of black holes in galaxy formation and evolution", A. Cattaneo, S. M. Faber, J. Binney, A. Dekel, J. Kormendy, R. Mushotzky, A. Babul, P. N. Best, M. Brüggen, A. C. Fabian, C. S. Frenk, A. Khalatyan, H. Netzer, A. Mahdavi, J. Silk, M. Steinmetz & L. Wisotzki; Nature 460, 213-219 (9 July 2009) doi:10.1038/nature08135]

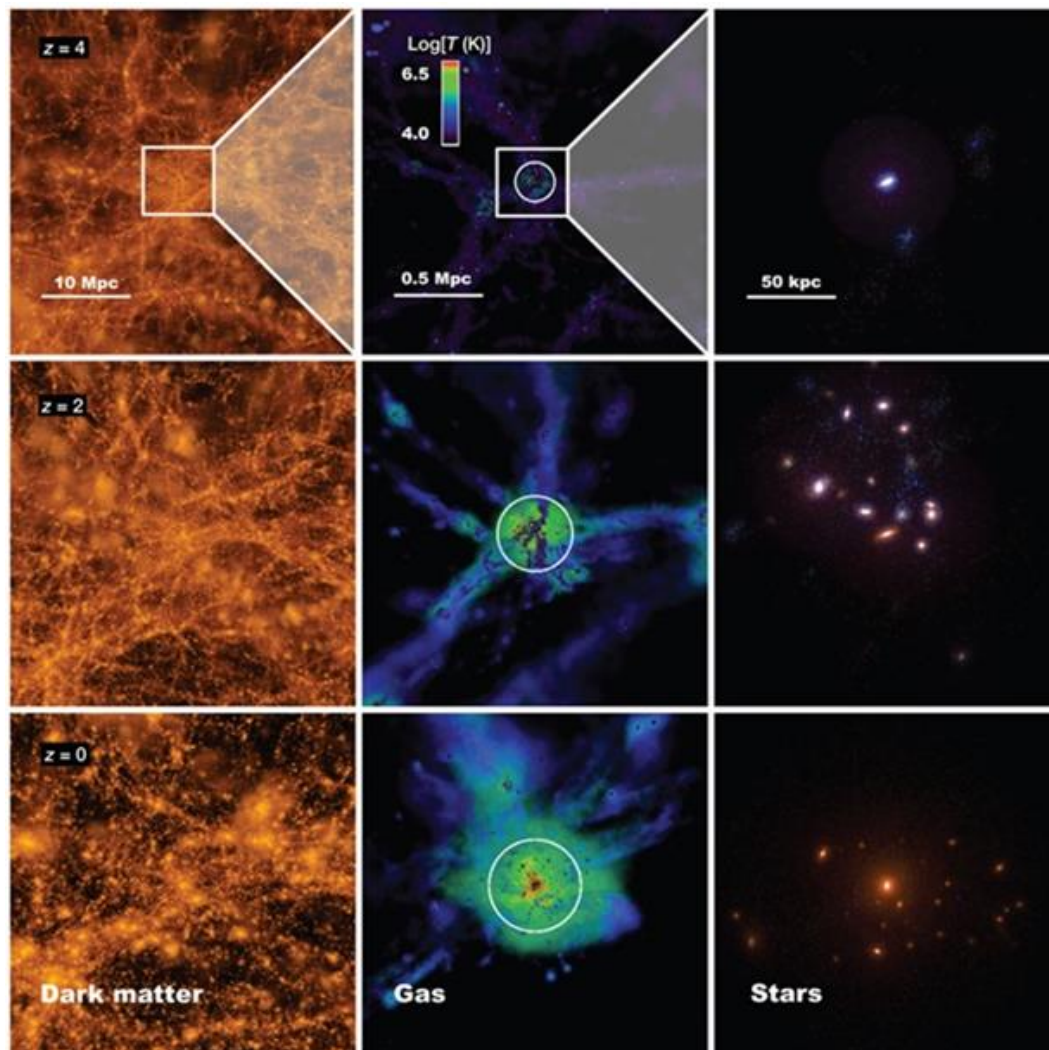


Figure C.2 A computer simulation of the formation of an elliptical galaxy. The nine panels illustrate the formation of an elliptical galaxy by showing how the dark matter (left column), the gas (centre column) and the stars (right column) are distributed at three epochs in the expansion of the Universe: when the Universe was 1/5 of its current size (redshift $z = 4$), when the Universe was 1/3 of its current size ($z = 2$), and today ($z = 0$). The gravity of the dark matter dominates the evolution on large scales (left column). As time passes, the Universe becomes lumpier because the dark matter clumps via gravity into haloes (bright orange spots in the left panels). The centre column zooms into the region around and inside a halo to show what happens to the gas. The halo radius is shown as a white circle, and the gas is colour-coded according to its temperature: blue is cold, green (and red) is hot. Initially the halo is small, and the gas streams into the halo down to its centre in cold flows. When the halo reaches the critical mass $M_{crit} \approx 10^{12} M_{\odot}$ ($z = 2$), the gas begins to form a hot atmosphere (green); eventually, all the gas within the halo is hot ($z = 0$). The right column zooms in even further to show the visible galaxy formed by the gas fallen to the centre. The galaxy is initially a blue spiral ($z = 4$). It starts to become red when the halo gas starts to be hot ($z = 2$). By then, its halo has merged with neighbouring haloes to form a galaxy group. Mergers with companions eventually transform the galaxy into an elliptical ($z = 0$). [ibid]

Acknowledgement

I acknowledge the cooperation extended by the Director, IIT, Patna, in letting me use the library facilities of his Central Library. This research is sponsored by University Grants Commission, India, under Emeritus Fellow Scheme.

References

1. Abell, G. O., Corwin Jr, H. G., & Olowin, R. P. (1989). A catalog of rich clusters of galaxies. *Astrophysical Journal Supplement Series (ISSN 0067-0049)*, vol. 70, May 1989, p. 1-138., 70, 1-138.
2. Bhattacharjee, Y. (2011). Milky Way Researchers' Home Away From Home.
3. Albrecht, A., & Steinhardt, P. J. (1982). Cosmology for grand unified theories with radiatively induced symmetry breaking. *Physical Review Letters*, 48(17), 1220.
4. Bardeen, J. M., Steinhardt, P. J., & Turner, M. S. (1983). Spontaneous creation of almost scale-free density perturbations in an inflationary universe. *Physical Review D*, 28(4), 679.
5. Benz, W., Slattery, W. L., & Cameron, A. G. W. (1986). The origin of the Moon and the single-impact hypothesis I. *Icarus*, 66(3), 515-535.
6. Benz, W., Slattery, W. L. & Cameron, A. G. W. "The Origin of the Moon & the Single Impact Hypothesis (3)," *ICARUS*, 71, 30-45, (1987).
7. Bennett, C. L., Bay, M., Halpern, M., Hinshaw, G., Jackson, C., Jarosik, N., ... & Wright, E. L. (2003). The microwave anisotropy probe* mission. *The Astrophysical Journal*, 583(1), 1.
8. Bennett, C. L., Larson, D., Weiland, J. L., Jarosik, N., Hinshaw, G., Odegard, N., ... & Wright, E. L. (2013). Nine-year Wilkinson Microwave Anisotropy Probe (WMAP) observations: final maps and results. *The Astrophysical Journal Supplement Series*, 208(2), 20.
9. Bethe, H. A. (1968). J. Robert Oppenheimer, 1904-1967.
10. Berardelli, Phil "The Mother of All Pileups", *ScienceNOW*, 17th April 2009;
11. Bloom, J. S., Giannios, D., Metzger, B. D., Cenko, S. B., Perley, D. A., Butler, N. R., ... & Van Der Horst, A. J. (2011). A possible relativistic jetted outburst from a massive black hole fed by a tidally disrupted star. *Science*, 333(6039), 203-206.
12. Bonta,E.D.;Ferrarese,L.;Corsini,E.M. et.al. "The Black Hole Mass of Abell1836-BCG and Abell3565-BCG", *Mem.S.A.It.* 78, 745 (2007), arXiv:0706.1959.
13. Dalla Bonta, E., Ferrarese, L., Miralda-Escudé, J., Coccato, L., Corsini, E. M., & Pizzella, A. (2006). Supermassive black holes in BCGs. *Proceedings of the International Astronomical Union*, 2(S238), 355-356.
14. van den Bosch, R. C., Gebhardt, K., Gültekin, K., van de Ven, G., van der Wel, A., & Walsh, J. L. (2012). An over-massive black hole in the compact lenticular galaxy NGC 1277. *Nature*, 491(7426), 729-731.
15. Boylan-Kolchin, M., Ma, C. P., & Quataert, E. (2006). Red mergers and the assembly of massive elliptical galaxies: the fundamental plane and its projections. *Monthly Notices of the Royal Astronomical Society*, 369(3), 1081-1089.
16. Bottches, M. "Modelling the emission processes in Blazers", *Astrophysics and Space Sciences*, 309, pp.95, (2007);
17. Braun, R. (2013). The cosmic web in focus. *Nature*, 497(7448), 191-192.
18. Brungendarf, J. & Meusinger,H; "The Galaxy Cluster ABELL 426 (Perseus)- A catalogue of 660 galaxy positions, isophotal magnitudes and morphological types", *Astronomy & Astrophysics Supplement*, v139, pp 144-161, 1999.
19. Cain, F. (2009). What Is Intergalactic Space? Universe Today Website.
20. Cain, Fraser, "New Evidence of Cold Dark Matter", *Universe Today*, June 12, (2003).
21. Cameron, A.G.W. "The Origin of the Moon & the Single Impact Hypothesis (5)," *ICARUS*, 126, 126-137, (1997).
22. Cameron, A. G. W. (2002). Birth of a solar system. *Nature*, 418(6901), 924-925.
23. Canup, R. M., & Esposito, L. W. (1996). Accretion of the Moon from an impact-generated disk. *Icarus*, 119(2), 427-446.
24. Canup, R. M., & Asphaug, E. (2001). Origin of the Moon in a giant impact near the end of the Earth's formation. *Nature*, 412(6848), 708-712.
25. Carlberg, J. K., Majewski, S. R., & Arras, P. (2009). The role of planet accretion in creating the next generation of red giant rapid rotators. *The Astrophysical Journal*, 700(1), 832.
26. Einasto, M., Einasto, J., Tago, E., Müller, V., & Andernach, H. (2001). Optical and X-ray clusters as tracers of the supercluster-void network. I. Superclusters of Abell and X-ray clusters. *The Astronomical Journal*, 122(5), 2222.
27. Cattaneo, A., Faber, S. M., Binney, J., Dekel, A., Kormendy, J., Mushotzky, R., ... & Wisotzki, L. (2009). The role of black holes in galaxy formation and evolution. *Nature*, 460(7252), 213-219.
28. Chapman, G. N. F., Geller, M. J., & Huchra, J. P. (1988). Linear clusters of galaxies-A194. *The Astronomical Journal*, 95, 999-1022.
29. Chincarini, G; Thompson, L.A.; Rood, H.J.; "Supercluster bridge between groups of galaxy clusters", *ApJ*, Part 2-Letter to the Editor, Oct 15, 1981, L47 -L50
30. Cho, A., & Stone, R. (2007). Racing to capture darkness. *Science*, 317(5834), 32-34.
31. Cho, A. (2013). Dark-Matter Mystery Nears Its Moment of Truth.
32. Conselice, Christopher J.;Gallagher, John S.; "Galaxy Aggregates in the COMA Cluster", *Monthly Notices of Royal Astronomical Society* 297(2), L34-L38, (1998)
33. Cook, C. L. (2004). Comment on 'Gravitational Slingshot', by Dukla JJ, Cacioppo, R., & Gangopadhyaya. *A.[American Journal of Physics*, 72 (5), pp 619-621.
34. Courtland, Rachel "Controversial dwarf planet finally named 'Haumea'." *New Scientist*, 18th September (2008)
35. Clery, Daniel "Galaxy Evolution", *Science*, 333, 173-175, 8th July (2011).
36. Cruzen, Shaun T.; Weistrop, Donna; Hoopes, Charles G; "Photometry of Galaxies in the Bootes Void", *ApJ*, v113, 1983
37. Cucchira,A., Levan, A.J., Fox, D.B., et.al. "A photometric redshift of $z \sim 9.4$ for GRB 090429B",*Ap.J.* accepted for

- publication, 2011
38. Da Costa, L. N., Numes, M. A., Pellegrini, P. S., Willmer, C., Chincarini, G., & Cowan, J. J. (1986). Redshift observations in the Centaurus-Hydra supercluster region. I. *Astronomical Journal* (ISSN 0004-6256), vol. 91, Jan. 1986, p. 6-12. *Research supported by the University of Oklahoma.*, 91, 6-12.
 39. da Costa, L.N.; William, C.; Pellegrini, P.S.; Chincarini, G.; “Red Shift observation in the Centaurus-Hydra Supercluster region II”, *Astronomical Journal*, v93, June 1987, pp.1338-1349;
 40. da Costa, L.Nicolai; Gellan, M.J.; Pellegrini, P.S.; et. al. ; “ A complete southern sky redshift survey,” *ApJ, Part 2 Letters*, v424, No.1, L1 to L4.
 41. Darwin, G. H. “On the precession of a viscous spheroid and on the remote history of the Earth,” *Philosophical Transactions of Royal Society of London*, Vol. 170, pp 447-530, (1879).
 42. Darwin, G. H. (1880). On the secular changes in the elements of the orbit of a satellite revolving about a planet distorted by tides. *Nature*, 21(532), 235-237.
 43. Di Nella, H., Couch, W. J., Paturel, G., & Parker, Q. A. (1996). Are the Perseus—Pisces chain and the Pavo—Indus wall connected?. *Monthly Notices of the Royal Astronomical Society*, 283(2), 367-380.
 44. Dukla, J.J., Cacioppo, R., & Gangopadhyaya, A. “Gravitational slingshot”, *American Journal of Physics*, 72(5), pp 619-621, May, (2004).
 45. Dunkley, J. Five-year Wilkinson microwave anisotropy probe (WMAP) observations: Likelihoods and parameters from the WMAP data (2008). *arXiv preprint arXiv:0803.0586*.
 46. Dunlop, James S. “The cosmic history of Star Formation”, *Science*, 333, 178-181, (2011).
 47. Dickey, J. O., Bender, P. L., Faller, J. E., Newhall, X. X., Ricklefs, R. L., Ries, J. G., ... & Yoder, C. F. (1994). Lunar laser ranging: A continuing legacy of the Apollo program. *Science*, 265(5171), 482-490.
 48. Dreyer, J.L.E., “*Tycho Brahe: A picture of Scientific Life and Work in Sixteenth Century*”, Kessinger Publication (2004).
 49. Einasto, M., Einasto, J., Tago, E., Andernach, H., Dalton, G. B., & Müller, V. (2002). Optical and X-ray clusters as tracers of the supercluster-void network. III. Distribution of Abell and APM clusters. *The Astronomical Journal*, 123(1), 51.
 50. Epstein, K. J. (2005). Shortcut to the slingshot effect. *American journal of physics*, 73(4), 362-362.
 51. Filippenko, A. V., & Riess, A. G. (1998). Results from the high-z supernova search team. *Physics Reports*, 307(1-4), 31-44.
 52. Fitchett, M., & Merritt, D. (1988). Dynamics of the Hydra I galaxy cluster. *Astrophysical Journal, Part 1* (ISSN 0004-637X), vol. 335, Dec. 1, 1988, p. 18-34., 335, 18-34.
 53. Fixsen, D. J. (2009). The temperature of the cosmic microwave background. *The Astrophysical Journal*, 707(2), 916.
 54. Fossati, G. A., Maraschi, L., Celotti, A., Comastri, A., & Ghisellini, G. (1998). A unifying view of the spectral energy distributions of blazars. *Monthly Notices of the Royal Astronomical Society*, 299(2), 433-448.
 55. Fritz, G., Davidson, A., Meekins, J.F., “Discovery of an X-Ray Source in Perseus”, *ApJ*. 164, pp.L81-85, March 15, (1971).
 56. Gale, T. Ptolemaic Astronomy, Islamic Planetary Theory and Copernican's Debt to the Maragha School. *Science and its Times*, 2005-2006.
 57. Genstenkorn, H. “Über Gezeitenreibung beim Zweikarpenproblem,” *Z. Astrophysics*, 26, 245-274, 1955.
 58. Goldreich, P. (1966). History of the lunar orbit. *Reviews of Geophysics*, 4(4), 411-439.
 59. Goldhaber, G., & Perlmutter, S. (1998). A study of 42 Type Ia supernovae and a resulting measurement of Ω_m and Ω_Λ . *Physics Reports*, 307(1-4), 325-331.
 60. Gomes, R., Levison, H. F., Tsiganis, K., & Morbidelli, A. (2005). Origin of the cataclysmic Late Heavy Bombardment period of the terrestrial planets. *Nature*, 435(7041), 466-469.
 61. Gregory, S.A. and Thompson, L.A., “ The COMA/A1367 supercluster and its environ”, *ApJ, Part 1*, v222, June 15, (1978), 784 – 799.
 62. Gregory, S. A., & Thompson, L. A. (1984). The A2197 and A2199 galaxy clusters. *Astrophysical Journal, Part 1* (ISSN 0004-637X), vol. 286, Nov. 15, 1984, p. 422-436., 286, 422-436.
 63. Gursky, H., Kellogg, E., Murray, S., Leong, C., Tananbaum, H., & Giacconi, R. (1971). A strong X-ray source in the Coma cluster observed by UHURU. *Astrophysical Journal*, vol. 167, p. L81, 167, L81.
 64. Guth, A. H. (1981). Inflationary universe: A possible solution to the horizon and flatness problems. *Physical Review D*, 23(2), 347.
 65. Guth, A. H., & Pi, S. Y. (1982). Fluctuations in the new inflationary universe. *Physical Review Letters*, 49(15), 1110.
 66. Hari S.E., Fabian A.C. & White D.A., “On the mass distribution in the Shapley Supercluster inferred from X-Ray Observations”, *Monthly Notices of Royal Astronomical Society*, v289, 787-800 (1997)
 67. Hawking, S. (Ed.). (2004). *The Illustrated on the shoulders of giants*. Running Press.
 68. Hawking, S. W. (1982). The development of irregularities in a single bubble inflationary universe. *Physics Letters B*, 115(4), 295-297.
 69. Heckman, T. M., & Kauffmann, G. (2011). The coevolution of galaxies and supermassive black holes: a local perspective. *science*, 333(6039), 182-185.
 70. Hellier, C., Anderson, D. R., Cameron, A. C., Gillon, M., Hebb, L., Maxted, P. F. L., ... & Wheatley, P. J. (2009). An orbital period of 0.94 days for the hot-Jupiter planet WASP-18b. *Nature*, 460(7259), 1098-1100.
 71. Hinshaw, G., Larson, D., Komatsu, E., Spergel, D. N., Bennett, C., Dunkley, J., ... & Wright, E. L. (2013). Nine-year Wilkinson Microwave Anisotropy Probe (WMAP) observations: cosmological parameter results. *The Astrophysical Journal Supplement Series*, 208(2), 19.
 72. Hogan, C. J. (1996). Primordial deuterium and the big bang. *SCIEnTiFiC AMERiCAN*, 275(6), 68-73.
 73. Hopkins, P. F., Bundy, K., Hernquist, L., & Ellis, R. S. (2007). Observational evidence for the coevolution of galaxy mergers, quasars, and the blue/red galaxy transition. *The Astrophysical Journal*, 659(2), 976.
 74. Ibata, R., & Gibson, B. (2007). “The Ghost of Galaxies Past”, *Scientific American*, 40-46.

75. Ida, S., Canup, R. M., & Stewart, G. R. (1997). Lunar accretion from an impact-generated disk. *Nature*, 389(6649), 353-357.
76. Ikebe, Y., Ohashi, T., Makishima, K., Tsuru, T., Fabbiano, G., Kim, D. W., ... & Kondo, H. (1992). X-ray study of NGC 1399 in the Fornax cluster of galaxies. *Astrophysical Journal, Part 2-Letters (ISSN 0004-637X)*, vol. 384, Jan. 1, 1992, p. L5-L8., 384, L5-L8.
77. Israelian, G., Santos, N. C., Mayor, M., & Rebolo, R. (2001). Evidence for planet engulfment by the star HD82943. *Nature*, 411(6834), 163-166.
78. Jackson, B., Barnes, R., & Greenberg, R. (2009). Observational evidence for tidal destruction of exoplanets. *The Astrophysical Journal*, 698(2), 1357.
79. Jackson, B., Greenberg, R., & Barnes, R. (2008). Tidal heating of extrasolar planets. *The Astrophysical Journal*, 681(2), 1631.
80. Jones, J. B. (2005). How does the slingshot effect work to change the orbit of a spacecraft?. *Scientific American*, 293(5), 116-116.
81. Jordán, A., Côté, P., West, M. J., Marzke, R. O., Minniti, D., & Rejkuba, M. (2004). Hubble space telescope observations of cD galaxies and their globular cluster systems. *The Astronomical Journal*, 127(1), 24.
82. Jordán, A., Blakeslee, J. P., Côté, P., Ferrarese, L., Infante, L., Mei, S., ... & West, M. J. (2007). The ACS Fornax Cluster Survey. I. Introduction to the survey and data reduction procedures. *The Astrophysical Journal Supplement Series*, 169(2), 213.
83. Kaula, W. M. (1964). Tidal dissipation by solid friction and the resulting orbital evolution. *Reviews of geophysics*, 2(4), 661-685.
84. Kazanas, D. (1980). Dynamics of the universe and spontaneous symmetry breaking. *The Astrophysical Journal*, 241, L59-L63.
85. Kerr, R. A. (2002). The first rocks Whisper of their origins.
86. Klypin, A., Hoffman, Y., Kravtsov, A. V., & Gottlöber, S. (2003). Constrained simulations of the real universe: The local supercluster. *The astrophysical journal*, 596(1), 19.
87. Komatsu, E., Smith, K. M., Dunkley, J., et.al. (2011). "Seven-Year Wilkinson Microwave Anisotropy Probe (WMAP) Observations: Cosmological Interpretation", *Astrophysical Journal Supplement*, 192, 18.
88. Kormendy, J., Bender, R., Magorrian, J., Tremaine, S., Gebhardt, K., Richstone, D., ... & Lauer, T. R. (1997). Spectroscopic evidence for a supermassive black hole in NGC 4486B. *The Astrophysical Journal*, 482(2), L139.
89. Kopylova, F. G., & Kopylov, A. I. (1998). Structure and dynamic state of the Corona Borealis supercluster. *Astronomy Letters*, 24, 491-496.
90. Kipp, M. E., Melosh, H. J. (1986). "Origin of the Moon," edited by Hartmann, Phillip and Taylor, 643-647, Publishers : Lunar & Planetary Sciences, Houston.
91. Krasinsky, G. A. (2002). Dynamical history of the Earth-Moon system. *Celestial Mechanics and Dynamical Astronomy*, 84, 27-55.
92. Krishner, Robert P., Oemler, Augustus. Jr., Schechter, Paul. L., Shectman, Stephan. A., "A survey of Bootes Void", *ApJ, Part 1*, v314, March 15, 1987, 493-506.
93. Kupperburg, Paul. (2005). "Hubble and the Big Bang", The Rosen Publishing House, 45-46, (2005).
94. Lawson, Russels, Burns, William Earl, (Editor) " Science in the Ancient World- An Encyclopaedia", *History of Science*, ABC-Chos, pp. 29-30, (2004)
95. Leschiutta, S., & Tavella, P. (2001, January). Reckoning time, longitude and the history of the earth's rotation, using the moon. In *Earth-Moon Relationships: Proceedings of the Conference held in Padova, Italy at the Accademia Galileiana di Scienze Lettere ed Arti*, November 8-10, 2000 (pp. 225-236). Dordrecht: Springer Netherlands.
96. Levan, A. J., Tanvir, N. R., Cenko, S. B., Perley, D. A., Wiersema, K., Bloom, J. S., ... & Xu, D. (2011). An extremely luminous panchromatic outburst from the nucleus of a distant galaxy. *Science*, 333(6039), 199-202.
97. Lewis, A. D., Buote, D. A., & Stocke, J. T. (2003). Chandra observations of a2029: The dark matter profile down to below 0.01 rvir in an unusually relaxed cluster. *The Astrophysical Journal*, 586(1), 135.
98. Linde, A. D. (1982). A new inflationary universe scenario: a possible solution of the horizon, flatness, homogeneity, isotropy and primordial monopole problems. *Physics Letters B*, 108(6), 389-393.
99. Lucey, J. R., Currie, M. J., & Dickens, R. J. (1986). The Centaurus cluster of galaxies-II. The bimodal velocity structure. *Monthly Notices of the Royal Astronomical Society*, 221(2), 453-472.
100. Lucey, J. R., & Carter, D. (1988). Distances to five nearby southern galaxy clusters and the absolute motion of the Local Group. *Monthly Notices of the Royal Astronomical Society*, 235(4), 1177-1201.
101. MacDonald, G. J. (1964). Tidal friction. *Reviews of Geophysics*, 2(3), 467-541.
102. Mahdavi, A., Geller, M. J., Fabricant, D. G., Kurtz, M. J., Postman, M., & McLean, B. (1996). The lumpy cluster abell 1185. *Astronomical Journal* v. 111, p. 64, 111, 64.
103. Chatzikos, M., Sarazin, C. L., & Kempner, J. C. (2006). Chandra observation of abell 2065: An unequal mass merger?. *The Astrophysical Journal*, 643(2), 751.
104. Maurellis, A., Fairall, A. P., Matrasers, D. R., & Ellis, G. F. R. (1990). A two-dimensional sheet of galaxies between two southern voids. *Astronomy and Astrophysics (ISSN 0004-6361)*, vol. 229, no. 1, March 1990, p. 75-79., 229, 75-79.
105. McConnell, N. J., Ma, C. P., Gebhardt, K., Wright, S. A., Murphy, J. D., Lauer, T. R., ... & Richstone, D. O. (2011). Two ten-billion-solar-mass black holes at the centres of giant elliptical galaxies. *Nature*, 480(7376), 215-218.
106. Mayer, L., Quinn, T., Wadsley, J., & Stadel, J. (2002). Formation of giant planets by fragmentation of protoplanetary disks. *Science*, 298(5599), 1756-1759.
107. Maraschi, L., & Tavecchio, F. (2003). The jet-disk connection and blazar unification. *The Astrophysical Journal*, 593(2), 667.
108. McNamara, B. R., & Nulsen, P. E. J. (2007). Heating hot atmospheres with active galactic nuclei. *Annu. Rev. Astron. Astrophys.*, 45, 117-175.
109. Melosh, H. J., & Kipp, M. E. (1989). *Lunar Planetary Science*

- Conference XX, 685-686.
110. Merritt, D. (1985). Relaxation and tidal stripping in rich clusters of galaxies. III-Growth of a massive central galaxy. *Astrophysical Journal, Part 1 (ISSN 0004-637X)*, vol. 289, Feb. 1, 1985, p. 18-32., 289, 18-32.
 111. Mieske, S., Hilker, M., Jordán, A., Infante, L., & Kissler-Patig, M. (2007). A search for ultra-compact dwarf galaxies in the Centaurus galaxy cluster. *Astronomy & Astrophysics*, 472(1), 111-119.
 112. Morbidelli, A., Levison, H. F., Tsiganis, K., & Gomes, R. (2005). Chaotic capture of Jupiter's Trojan asteroids in the early Solar System. *Nature*, 435(7041), 462-465.
 113. Mukhanov, V. F., & Chibisov, G. V. (1981). Quantum fluctuations and a nonsingular universe. *ZhETF Pisma Redaktsiiu*, 33, 549-553.
 114. NASA/IPAC Extra Galactic DataBase(NED) operated by Jet Propulsion Laboratory, California Institute of Technology under contract with NASA.
 115. Nakazawa, K., Makishima, K., Fukazawa, Y., & Tamura, T. (2000). ASCA Observations of a Near-by Cluster in Antlia. *Publications of the Astronomical Society of Japan*, 52(4), 623-630.
 116. McConnell, N. J., Ma, C. P., Gebhardt, K., Wright, S. A., Murphy, J. D., Lauer, T. R., ... & Richstone, D. O. (2011). Two ten-billion-solar-mass black holes at the centres of giant elliptical galaxies. *Nature*, 480(7376), 215-218.
 117. Optical Gravitational Lensing Experiment (OGLE) Collaboration Udalski A. 13 Szymański MK 13 Kubiak M. 13 Pietrzyński G. 13 14 Poleski R. 13 Soszyński I. 13 Wyrzykowski Ł. 15 Ulaczyk K. 13. (2011). Unbound or distant planetary mass population detected by gravitational microlensing. *Nature*, 473(7347), 349-352.
 118. Panter, B., Jimenez, R., Heavens, A. F., & Charlot, S. (2007). The star formation histories of galaxies in the Sloan Digital Sky Survey. *Monthly Notices of the Royal Astronomical Society*, 378(4), 1550-1564.
 119. Pastorello, A., & Patat, F. (2008). Echo from an ancient supernova. *Nature*, 456(7222), 587-589.
 120. Petit, J. M., Kavelaars, J. J., Gladman, B. J., Margot, J. L., Nicholson, P. D., Jones, R. L., ... & Taylor, P. A. (2008). The extreme Kuiper belt binary 2001 QW322. *Science*, 322(5900), 432-434.
 121. Peebles, P. J. E., Schramm, D. N., Turner, E. L., & Kron, R. G. (1994). The evolution of the universe. *Scientific American*, 271(4), 52-57.
 122. Peebles, P. J. E., Page, L. A., & Partridge, R. B. (2009). *Finding the big bang*. Cambridge University Press.
 123. Penzias, A.A. & Wilson, R.W. *ApJ*, 142,419 (1965)
 124. Postman, M., Geller, M. J., & Huchra, J. P. (1988). The dynamics of the Corona Borealis supercluster. *Astronomical Journal (ISSN 0004-6256)*, vol. 95, Feb. 1988, p. 267-283., 95, 267-283.
 125. Pisanti, O., Cirillo, A., Esposito, S., Iocco, F., Mangano, G., Miele, G., & Serpico, P. D. (2008). PArthENoPE: Public algorithm evaluating the nucleosynthesis of primordial elements. *Computer Physics Communications*, 178(12), 956-971.
 126. Pringle. (1981). "Eddington Accretion", *Annual Review Astronomy and Astrophysics*, 19, sec 1-4.
 127. Purcell, C. W., Bullock, J. S., Tollerud, E. J., Rocha, M., & Chakrabarti, S. (2011). The Sagittarius impact as an architect of spirality and outer rings in the Milky Way. *Nature*, 477(7364), 301-303.
 128. Rubicam, D. P. (1975). "Tidal Friction & the Early History of Moon's Orbit", *Journal of Geophysical Research*, 80(11), 1537-1548.
 129. van den Bosch, R. C., Gebhardt, K., Gültekin, K., van de Ven, G., van der Wel, A., & Walsh, J. L. (2012). An over-massive black hole in the compact lenticular galaxy NGC 1277. *Nature*, 491(7426), 729-731.
 130. Reichardt, C. L., Shaw, L., Zahn, O., Aird, K. A., Benson, B. A., Bleem, L. E., ... & Williamson, R. (2012). A measurement of secondary cosmic microwave background anisotropies with two years of South Pole Telescope observations. *The Astrophysical Journal*, 755(1), 70.
 131. Reynolds, C. S. (2008). Bringing black holes into focus. *Nature*, 455(7209), 39-40.
 132. Sharma, B. K. (2023). Fractal Architecture of the Universe Based on Primary-Centric World-View-A Post Co-pernican Conjecture. *J Math Techniques Comput Math*, 2(12), 504-574.
 133. Santos, N. C., Benz, W., & Mayor, M. (2005). Extrasolar planets: constraints for planet formation models. *Science*, 310(5746), 251-255.
 134. Sato, K. (1981). First-order phase transition of a vacuum and the expansion of the Universe. *Monthly Notices of the Royal Astronomical Society*, 195(3), 467-479.
 135. Schilling, G. (2001). The first split second. *New Scientist*, 169(2284), 26-9.
 136. Schödel, R., Ott, T., Genzel, R., Hofmann, R., Lehnert, M., Eckart, A., ... & Menten, K. M. (2002). A star in a 15.2-year orbit around the supermassive black hole at the centre of the Milky Way. *Nature*, 419(6908), 694-696.
 137. Semeniuk, Ivan. (2008). "Huge haul of Earth-like planets found", *New Scientist*.
 138. Seife, C. (2003). Illuminating the dark universe.
 139. Sharma, B., & Ishwar, B. (2002). Lengthening of day (lod) curve could be experiencing chaotic fluctuations with implications for earthquake predictions. In *34th COSPAR Scientific Assembly* (Vol. 34, p. 3078).
 140. Sharma, B. K., & Ishwar, B. (2004a). "Planetary Satellite Dynamics : Earth-Moon, Mars-Phobos-Deimos and Pluto-Charon (Parth-I)" *35th COSPAR Scientific Assembly*, 18-25th July (2004a), Paris, France
 141. Sharma, B. K., & Ishwar, B. (2004b). "A New Perspective on the Birth and Evolution of our Solar System based on Planetary Satellite Dynamics", *35th COSPAR Scientific Assembly*, 18-25th July (2004b), Paris, France.
 142. Sharma, B. K. & Ishwar, B., (2004c). "Jupiter-like Exo-Solar Planets confirm the Migratory Theory of Planets" *Recent Trends in Celestial Mechanics-2004*, pp.225-231, BRA Bihar University, 1st – 3rd November (2004c), Muzaffarpur, Bihar. Publisher Elsevier.
 143. Sharma, B. K. (2008). Basic Mechanics of Planet-Satellite Interaction with special reference to Earth-Moon System. *arXiv preprint arXiv:0805.0100*.

144. Sharma, B.K. (2008b) personal communication, "Theoretical Formulation of Phobos, moon of Mars, rate of altitudinal loss", <http://arXiv.org/abs/0805.0454>.
145. Sharma, B.K., personal communication, "Theoretical formulation of the origin of cataclysmic late heavy bombardment era based on the new perspective of birth and evolution of solar systems", <http://arXiv.org/abs/0807.5093>, (2008c)
146. Sharma, B. K., Ishwar, B., & Rangesh, N. (2009). Simulation software for the spiral trajectory of our Moon. *Advances in space research*, 43(3), 460-466.
147. Sharma, B. K. (2011). The Architectural Design Rules of Solar Systems Based on the New Perspective. *Earth, Moon, and Planets*, 108, 15-37.
148. Silvestrini, S., Krizman, C., Ceretti, G. et.al. "Analysis of Abell 779-photometry and spectroscopy of the cluster", *II Cido come Laboratorio*, 1 A.S 2010-2011.
149. Sievers, J. L., Hlozek, R. A., Nolte, M. R., Acquaviva, V., Addison, G. E., Ade, P. A., ... & Zunckel, C. (2013). The Atacama Cosmology Telescope: Cosmological parameters from three seasons of data. *Journal of Cosmology and Astroparticle Physics*, 2013(10), 060.
150. Smoot, G. F., Gorenstein, M. V., & Muller, R. A. (1977). Detection of anisotropy in the cosmic blackbody radiation. *Physical Review Letters*, 39(14), 898.
151. Smoot, G. F., Bennett, C. L., Kogut, A. et.al. (1992). " *ApJ*, 396, L1.
152. Spergel, D.N.; Vergel, L.; Peiris, H.V.; et.al. " ", *ApJS*, 148, 175, [arXiv astro-ph/0302209](http://arXiv.org/astro-ph/0302209) (2003);
153. Srinivasan, G. (Ed.). (2000). *From white dwarfs to black holes: the legacy of S. Chandrasekhar*. University of Chicago Press.
154. Steinmetz et.al. "Huge elliptical galaxy of 13th Magnitude", [arXiv:astro-ph/0606211](http://arXiv.org/astro-ph/0606211).v1
155. Starobinsky, A. A. (1979). *ZhETF Pis ma Redaktsiiu*, 30, 719.
156. Starobinsky, A. A. (1982). Dynamics of phase transition in the new inflationary universe scenario and generation of perturbations. *Physics Letters B*, 117(3-4), 175-178.
157. Story, K. T., Reichardt, C. L. Hou, Z.; et.al. (2012). e-print 1210.7231.
158. Tallin, Estonian SSR. (1978). "The Large Scale Structure of the Universe", *Proceedings of the Symposium*, Sept 12-16, 1977; Publishing Co., pp 241-250, discussion 250, 251.
159. Tarenghi, M., Tifft, W. G., Chincarini, G., Rood, H. J., & Thompson, L. A. (1979). The Hercules supercluster. I-Basic data. *Astrophysical Journal, Part 1*, vol. 234, Dec. 15, 1979, p. 793-801., 234, 793-801.
160. Tarenghi, M., Chincarini, G., Rood, H. J., & Thompson, L. A. (1980). The Hercules supercluster. II-Analysis. *Astrophysical Journal, Part 1*, vol. 235, Feb. 1, 1980, p. 724-742., 235, 724-742.
161. Tolstoy, E. (2011). Galactic paleontology. (6039), 176-178.
162. Töuma, J., & Wisdom, J. (1998). Resonances in the early evolution of the Earth-Moon system. *The Astronomical Journal*, 115(4), 1653.
163. Thomas, S. A., Abdalla, F. B., & Lahav, O. (2011). Excess clustering on large scales in the MegaZ DR7 photometric redshift survey. *Physical review letters*, 106(24), 241301.
164. Tsiganis, K., Gomes, R., Morbidelli, A., & Levison, H. F. (2005). Origin of the orbital architecture of the giant planets of the Solar System. *Nature*, 435(7041), 459-461.
165. Tully, R. B. (1982). The local supercluster. *Astrophysical Journal, Part 1*, vol. 257, June 15, 1982, p. 389-422., 257, 389-422.
166. Tully, R. B. (1982). Unscrambling the Local Supercluster. *Sky and Telescope*, 63, 550.
167. Tully, R. B., & Fisher, J. R. (1977). A new method of determining distances to galaxies. *Astronomy and Astrophysics*, vol. 54, no. 3, Feb. 1977, p. 661-673., 54, 661-673.
168. Ulrich, M. H., Maraschi, L., & Urry, C. M. (1997). Variability of active galactic nuclei. *Annual Review of Astronomy and Astrophysics*, 35(1), 445-502.
169. Uson, J. M., Boughn, S. P., & Kuhn, J. R. (1990). The central galaxy in Abell 2029: an old supergiant. *Science*, 250(4980), 539-540.
170. Urry, C. M. (1998). BL Lac Objects and Blazars: Past, Present, and Future. *arXiv preprint astro-ph/9812420*.
171. Vander, Bergh. (2000). Sidney ; "Updated Information of the Local Group", *the Publications of the Astronomical Society of the Pacific*, 112(770), 529-536,
172. Walker, S. A., Fabian, A. C., Sanders, J. S., George, M. R., & Tawara, Y. (2012). X-ray observations of the galaxy cluster Abell 2029 to the virial radius. *Monthly Notices of the Royal Astronomical Society*, 422(4), 3503-3515.
173. Walsh, K. J., Richardson, D. C., & Michel, P. (2008). Rotational breakup as the origin of small binary asteroids. *Nature*, 454(7201), 188-191.
174. Ward, W. R., & Canup, R. M. (2000). Origin of the Moon's orbital inclination from resonant disk interactions. *Nature*, 403(6771), 741-743.
175. Williams, G. E. (2000). Geological constraints on the Precambrian history of Earth's rotation and the Moon's orbit. *Reviews of Geophysics*, 38(1), 37-59.
176. Wolfe, S. A., Pisano, D. J., Lockman, F. J., McGaugh, S. S., & Shaya, E. J. (2013). Discrete clouds of neutral gas between the galaxies M31 and M33. *Nature*, 497(7448), 224-226.
177. Yuan, F., Quataert, E., & Narayan, R. (2003). Nonthermal electrons in radiatively inefficient accretion flow models of Sagittarius A. *The Astrophysical Journal*, 598(1), 301.
178. Zwicky, F. (1937). On the Masses of Nebulae and of Clusters of Nebulae. *apj*, 86: 217.

Copyright: ©2024 Bijay Kumar Sharma. This is an open-access article distributed under the terms of the Creative Commons Attribution License, which permits unrestricted use, distribution, and reproduction in any medium, provided the original author and source are credited.